Transition-Metal Derivatives of the Cyclopentadienylphosphine Bridging Unit: VI-Oxidation, Oxidative Addition, Insertion, and Metal–Metal Bond Formation in Dirhodium Complexes†

Xiaodong He, André Maisonnat, Françoise Dahan, and René Poilblanc*

Laboratoire de Chimie de Coordination du CNRS, UP 8241 liée par conventions à l'Université Paul Sabatier et à l'Institut National Polytechnique, 205 route de Narbonne, 31077 Toulouse Cedex, France

Received December 26, 1990

As part of our interest in bimetallic activation processes, the reactions of oxidative addition to the dinuclear (cyclopentadienyldiphenylphosphine)rhodium and -iridium complexes $[M^{I}(\mu\text{-}CpPPh_2)(CO)]_2$ (M = Rh (**1**) Ir (**12**)) have been studied. The two-electron direct chemical oxidation of **1** with ferrocenium or silver hexafluorophosphate allowed the preparation of a series of Rh^{II}–Rh^{II} cationic species, $[Rh^{II}L(\mu\text{-}CpPPh_2)]_2^{2+}$ (L = CO (**2a**), pyridine (**2b**), acetonitrile (**2c**), $P(OMe)_3$ (**2d**)). An X-ray diffraction study of the cationic dinuclear species **2b** revealed a drastic configurational change that does authorize a metal–metal bond formation (Rh–Rh distances equal to 4.3029 (6) Å in **1** and to 2.7796 (9) Å in **2b**) with subsequent cisoid disposition of the pyridine ligands. Also, oxidative addition reactions to **1**, of the most typical electrophiles, have been studied. With iodomethane, **1** leads to both mono- and biaddition products, $[Rh^{III}(CH_3CO)(I)(\mu\text{-}CpPPh_2)_2Rh^{I}(CO)]$ (**3**) and $[Rh^{III}(CH_3CO)(I)(\mu\text{-}CpPPh_2)]_2$ (**4**), depending on the CH_3I:Rh ratio used. The reaction with methyl triflate allowed the formation of the 1:1 electrolyte $[(CH_3CO)Rh^{II}(\mu\text{-}CpPPh_2)_2Rh^{II}(CO)]CF_3SO_3$ (**5a**), from which crystals of the hexafluorophosphate **5a′** were obtained. The X-ray diffraction study of **5a′** showed that it also adopted the configuration allowing the formation of a metal–metal bond (Rh–Rh = 2.7319 (6) Å). Thus, the pathway from **1** to **5** appears as the second example of a metal-promoted alkyl migration in dinuclear complexes. Further transformation of **5** to **3** by nucleophilic attack of iodide on the rhodium atom bearing the acetyl group was also observed and shown to imply the breaking of the metal–metal bond. The reaction of **1** with iodine leads, depending on the stoichiometry, to the formation of both the mono- and bisubstitution products, $[(I)_2Rh^{III}(\mu\text{-}CpPPh_2)_2Rh^{I}(CO)]$ (**6a**) and $[Rh^{III}(I)_2(\mu\text{-}CpPPh_2)]_2$ (**7a**), respectively; these compounds were fully identified by their spectroscopic data. With chlorine, the precipitation of $[(Cl)_2Rh^{III}(\mu\text{-}CpPPh_2)_2Rh^{I}(CO)]$ (**6b**) is observed together with the formation of a green solution from which the cationic species $[ClRh^{II}(\mu\text{-}CpPPh_2)_2Rh^{II}(CO)]^+$ (**8b**) was readily precipitated as the hexafluorophosphate. Infrared and NMR spectroscopic arguments allow us to propose for the cationic species **8** a metal–metal-bonded structure analogous to that of **5**. Reaction of **8** with nucleophiles, namely iodide or chloride, led to the metal–metal bond breaking, leading to species of type **6** (Rh^{III}, Rh^{I}). Starting with **2a**, the nucleophilic attack of the halides X^- led also to the monocationic intermediates $[XRh(\mu\text{-}CpPPh_2)_2Rh(CO)]^+$ (**8**) then to the formation of dihalo complexes **6**. In contrast, the reaction of the solvated cationic species $[Rh^{II}(solv)(\mu\text{-}CpPPh_2)]_2^{2+}$ (**2e**) with halides allowed the preparation of symmetric dihalo compounds $[Rh^{II}X(\mu\text{-}CpPPh_2)]_2$ (X = I (**9a**), or Cl (**9b**)). By studying the reactions of the tetraiodo complex (Rh^{III}–Rh^{III}), **7a**, and of the diiodo complex (Rh^{II}–Rh^{II}), **9a**, with the borohydride $LiBHEt_3$, spectroscopic evidence for the formation of hydrido derivatives was obtained. Reaction of **9a** with methyl- or phenyllithium afforded the preparation of the methyl or phenyl derivatives $[Rh^{II}(R)(\mu\text{-}CpPPh_2)]_2$ (R = Me (**10a**), or Ph (**10b**)). The intermediate species $[(CH_3)Rh^{II}(\mu\text{-}CpPPh_2)_2Rh^{II}(I)]$ (**11**) was also prepared and studied by X-ray diffraction (Rh–Rh = 2.7160 (7) Å). A comparison of the molecular structures of the metal–metal-bonded dication **2b**, monocationic **5a′**, and neutral **11** species is developed with reference to the related structure of **1**. In addition the general features of the novel $[M(\mu\text{-}CpPR_2]_2$ (R = Ph, Me) bridging unit are summed up and discussed in the context of a short review (presented in the Introduction) on the oxidative addition reactions involving bridged bimetallic complexes.

Introduction

Oxidative addition is probably the most characteristic reaction of the electron-rich metal complexes. As a decisive step in most catalytic processes, it always attracts unflagging attention. In this context, it is hoped that better knowledge of this reaction pathway in the case of bimetallic complexes will bring interesting insight into the potential of these species to solve difficult problems such as the activation of rather inert molecules. A valuable question that arises is knowing at what point the pathway of the reaction is subordinated to the molecular structure and/or to the nature of the metal site. From this point of view, we are presently exploring the reactivity of several series of homobimetallic derivatives utilizing the ligands $Cp_{(r)}PR_2$ ($Cp_{(r)}$ = C_5H_4, C_5Me_4, ...; R = CH_3, t-C_4H_9, Ph) as novel bridging units.[1c,d] These ligands have already been used in the synthesis of both homobimetallic and heterometallic complexes.[1a,b]

Actually, the oxidative addition, with di- or polymetallic complexes,[2] may occur on one or several sites, as shown schematically in Figure 1.

In so far as the mechanisms are concerned, the direct path from A to B or from B to D is rare, especially with symmetrical substrates that afford homolytic reactions. In such cases, the formation of C is generally first observed, then C transforms to B through the migration (v) of Y.

† Two preliminary communications[1c,d] on parts of this work have been recently published.

(1) (a) Bullock, M. R.; Casey, C. P. *Acc. Chem. Res.* **1987**, *20*, 167. (b) He, X. D.; Maisonnat, A.; Dahan, F.; Poilblanc, R. *Organometallics* **1989**, *8*, 2618. (c) He, X. D.; Maisonnat, A.; Dahan, F.; Poilblanc, R. *J. Chem. Soc., Chem. Commun.* **1990**, 671. (d) He, X. D.; Maisonnat, A.; Dahan, F.; Poilblanc, R. *New J. Chem.* **1990**, *14*, 313.

(2) Collman, J. P.; Hegedus, L. S.; Norton, J. R.; Finke, R. G. *Principles and Applications of Organotransition Metal Chemistry*; University Science Books: Mill Valley, CA, 1987; p 279.

0276-7333/91/2310-2443$02.50/0

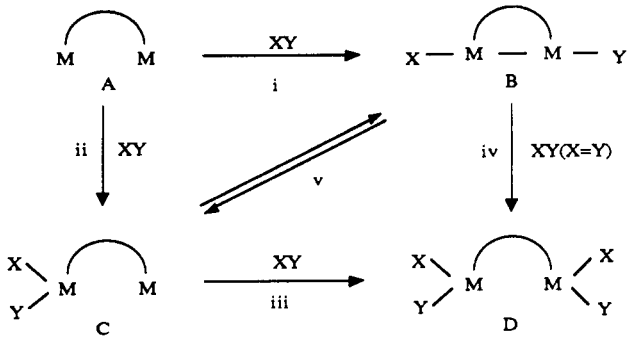

Figure 1. Possible pathways of the oxidative addition reactions on dimetallic complexes.

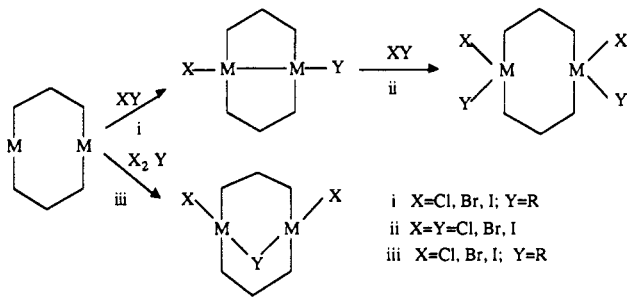

Figure 2. Representative examples of oxidative addition reactions on bimetallic "ylide" or dppm bridge complexes. [MM] = [AuAu]: $Au_2[(CH_2)_2PMe_2]_2$, $Au_2[(CH_2)_2PPh_2]_2$, $Au_2[CH_2P(S)Ph_2]_2$.[3] [MM] = [RhRh]: $Rh_2(CNCH_2CH_2CH_2NC)_4^{2+}$, $Rh_2(dppm)_2(CNR)_4^{2+}$, $Rh_2(dpam)_2(CO)_2Br_2$, $Rh_2(dppm)_2(CO)_2Cl_2$, $Rh_2(dpam)_2(CNR)_4^{2+}$, $Rh_2(dppm)_2(\mu\text{-dmpz})(CO)_2^{+}$.[4a-d] [MM] = [PdPd], [PtPt]: $Pd_2(dppm)_3$, $Pt_2(dppm)_3$.[4e,f,5]

Likewise, D is obtained from B, via C (vide infra). On the contrary, the direct pathway (i) may be observed with electrophiles XY, which undergo heterolytic cleavage.

Upon referring to the work of Schmidbaur,[3] Balch,[4] and Puddephatt,[5] it may be noticed that the bimetallic "ylide" complexes of gold and the dppm-bridged "face-to-face" complexes of rhodium, palladium, and platinum afford, without exception, oxidative addition of type (i) with the usual electrophiles, halogens (X_2) and alkyl halides (RX). Thus, for instance, the reaction of methyl iodide with the dinuclear gold complex $Au_2[(CH_2)_2PME_2]_2$ first observed by Schmidbaur and Francke in 1975,[3a] leads to a complex bearing the methyl and iodine groups on different centers and possessing a metal–metal bond. Some representative examples of such reactions are shown in Figure 2 with related references.

It is obvious that this type of "transannular" oxidative addition can occur only if the potential for interaction does exist between the two metal sites as a result of the structural characteristics of the complex. In many cases, this interaction seems to exist in the initial state of the complex, as demonstrated by Hoffmann on the grounds of EHMO calculations[6] in the case of, for instance, Au_2^{2+}. This is also the case for rhodium, palladium, and platinum complexes where the "face-to-face" arrangement of the square-planar coordination sphere planes allows (as shown by electronic spectroscopy and explained by theoretical analysis[4a,b,c,7-10]) various orbitals to overlap.

By comparison, another type of dinuclear square-planar complex, namely $[M(\mu\text{-}A)LL']_2$ (M = Rh or Ir), offers a completely different behavior. Actually, as shown for the rhodium chloro complexes (A = Cl, L = L' = CO) from ab initio calculations,[11] the geometry of their initial reactive state presumably does not allow any metal–metal interaction but the flexibility of the structure along the A–A axis affords interesting possibilites, especially when thiolato groups are used as bridging ligands A. In particular, this flexibility plays a major role in the *homolytic* oxidative addition of molecular hydrogen, which has been shown[12] to follow up pathways ii, v, or ii, iii (Figure 1) affording respectively di- or tetrahydrido derivatives, depending on the nature of the starting material (L = CO, L' = $P(OCH_3)_3$; L = CO, L' = $P(OBu)_3$).

More closely related to the present work, the heterolytic reactions of the alkyl halides[13,14] CH_3X (X = I, Br, Cl) with the complexes $[Rh^I(\mu\text{-Cl})(CO)(PR_3)]_2$ (R_3 = $(OMe)_3$, $PhMe_2$) afford the tetrahalo methyl complexes $[Rh^{III}Cl(CO)(PR_3)(CH_3)(X)]_2$ (X = Br, Cl) and acetyl complexes $[Rh^{III}Cl(COCH_3)(PR_3)(X)]_2$ (X = I). These reactions duplicate on both metal centers, the classical oxidative addition observed on mononuclear complexes. In contrast, when the same reaction is performed but using *tert*-butanethiolato groups as bridging ligands, CH_3I or CH_3Br in the molar ratio CH_3X:Rh = 1:2, it affords with the addition to one metal site only followed by methyl migration giving the acetyl dissymmetrical product, $[(COMe)(PR_3)Rh^{III}(\mu\text{-S-}t\text{-Bu})_2Rh^I(CO)(PR_3)]$.[13] Moreover, with the iridium homologous complexes, the same type of reaction leads to products of transannular oxidative addition, $[X(CO)PR_3Ir^{II}(\mu\text{-S-}t\text{-Bu})_2Ir^{II}Y(CO)PR_3]$ (X = Y = I;[14] X = I, Y = CH_3[15]). The different results observed with rhodium and iridium are explained by different states of polarity in the proposed cationic intermediate $[(CH_3)(CO)(PR_3)M^1(\mu\text{-S-}t\text{-Bu})_2M^2(CO)(PR_3)]^+$. The cationic charges are localized on the first reacting metal site, M^1, for rhodium, whereas for iridium, it is delocalized on the second one, M^2, presumably owing to metal–metal interaction in the transition state.

(3) (a) Schmidbaur, H.; Franke, R. *Inorg. Chim. Acta* **1975**, *13*, 85. (b) Schmidbaur, H.; Mandl, J. R.; Frank, A.; Huttner, G. *Chem. Ber.* **1976**, *109*, 466. (c) Schmidbaur, H.; Mandl, J. R.; Wagner, F.; Van de Vondel, D. F.; Van der Kelen, G. P. *J. Chem. Soc., Chem. Commun.* **1976**, 170. (d) Schmidbaur, H. *Acc. Chem. Res.* **1975**, *8*, 62. (e) Schmidbaur, H. *Angew. Chem., Int. Ed. Engl.* **1983**, *22*, 907. (f) Schmidbaur, H.; Pollok, Th.; Wagner, F. E.; Bau, R.; Riede, J.; Müller, G. *Organometallics* **1986**, *5*, 566.

(4) (a) Balch, A. L. *J. Am. Chem. Soc.* **1976**, *98*, 8049. (b) Balch, A. L.; Tulyathan, B. *Inorg. Chem.* **1977**, *16*, 2840. (c) Balch, A. L.; Labadie, J. W.; Delker, G. *Inorg. Chem.* **1979**, *18*, 1224. (d) Balch, A. L. In *Reactivity of metal-metal bonds*: ACS Symposium Series No. 155; American Chemical Society: Washington, DC, 1981; p 167. (e) Hunt, C. T.; Balch, A. L. *Inorg. Chem.* **1981**, *20*, 2267. (f) Balch, A. L.; Hunt, C. T.; Lee, C. L.; Olmstead, M. M.; Farr, J. P. *J. Am. Chem. Soc.* **1981**, *103*, 3764.

(5) (a) Puddephatt, R. *J. Chem. Soc. Res.* **1983**, 99. (b) Azam, K. A.; Puddephatt, R. J.; Brown, M. P.; Yavari, A. *J. Organomet. Chem.* **1982**, *234*, C31. (c) Azam, K. A.; Brown, M. P.; Hill, R. H.; Puddephatt, R. J.; Yavari, A. *Organometallics* **1984**, *3*, 697.

(6) Jiang, W. J.; Alvarez, S.; Hoffmann, R. *Inorg. Chem.* **1985**, *24*, 749.

(7) Lewis, N. S.; Mann, K. R.; Gordon, J. G., II; Gray, H. B. *J. Am. Chem. Soc.* **1976**, *98*, 7461.

(8) Oro, L. A.; Carmona, D.; Perez, P. L.; Esteban, M. *J. Chem. Soc., Dalton Trans.* **1985**, 973.

(9) Grossel, M.; Brown, M. P.; Nelson, C. D.; Yavari, A.; Kallas, E.; Moulding, R. P.; Seddon, K. R. *J. Organomet. Chem.* **1982**, *232*, C13.

(10) (a) Milder, S. J.; Goldberg, R. A.; Kliger, D. S.; Gray, H. *J. Am. Chem. Soc.* **1980**, *102*, 6761. (b) Rice, S. F.; Gray, H. *J. Am. Chem. Soc.* **1981**, *103*, 1593. (c) Dallinger, R. F.; Miskowski, V. M.; Gray, H. B.; Woodruff, W. H. *J. Am. Chem. Soc.* **1981**, *103*, 1595.

(11) Serafini, A.; Poilblanc, R.; Labarre, J. F.; Barthelat, J. C. *Theoret. Chim. Acta* **1978**, *50*, 159.

(12) (a) Bonnet, J. J.; Thorez, A.; Maisonnat, A.; Galy, J.; Poilblanc, R. *J. Am. Chem. Soc.* **1979**, *101*, 5904. (b) Guilmet, E.; Maisonnat, A.; Poilblanc, R. *Organometallics* **1983**, *2*, 1127.

(13) Mayanza, A.; Bonnet, J. J.; Galy, J.; Kalck, Ph.; Poilblanc, R. *J. Chem. Res., Synop.* **1980**, 146.

(14) Bonnet, J. J.; Kalck, Ph.; Poilblanc, R. *Angew. Chem.* **1980**, *92*, 572.

(15) El Amane, M.; Maisonnat, A.; Dahan, F.; Poilblanc, R. *New J. Chem.* **1988**, *12*, 661.

Similar observations were also extended by Stobart et al.[16] to the reaction of analogous pyrazolyl (pyrazole:pzH) bridged complexes with the electrophiles XY (XY = I_2 or CH_3I). Surprisingly, when the terminal ligands LL′ are bulky enough to preclude the formation of a "normal" metal–metal bond (e.g. when LL′ = 1,5-cyclooctadiene (cod)), the X and Y groups still coordinate to both iridium centers, giving products of the type $[(cod)XIr^{II}(\mu\text{-}pz)_2Ir^{II}(cod)Y]$ (X = Y = I; X = CH_3, Y = I) with large metal–metal distances.

With bimetallic complexes possessing parallel z metal orbitals, only classical oxidative additions are observed either on one center or on both metal centers leading to $M^{III}M^{I}$ or to $M^{III}M^{III}$ dimers, respectively. This is the case for both the rigid $[M_2L_2(PNNP)(\mu\text{-}PPh_2)]$ derivatives (PNNP = 3,5-bis(diphenylmethylene)pyrazolyl; M = Rh, Ir; L = CO)[17] and the $[Me_2Pt(\mu\text{-bpym})]_2$ derivative of bpym (2,2′-bipyrimidine)[18] or for *cis*-$[Me_2Pt(\mu\text{-}R_2PCH_2PR_2)]_2$ (R = Me, Ph),[19] which presents a chair conformation.

The last category of complexes to be considered consists of the cyclopentadienyl bimetallic complexes studied by Werner et al. and by Faraone et al. With the complex $CH_2[CpRh(PMe_3)L]_2$, Werner has observed simple duplication of the oxidative addition of the methyl carbocation CH_3^+ or of CH_3I.[20] Similar results were described by Faraone for the complex $[CpRh(CO)]_2(\mu\text{-dppb})$[21] built around the bridging ligand dppb (bis(diphenylphosphino)butane). Oxidative addition of the electrophiles X_2, CH_3^+, CH_3I is the same as that observed in the monometallic $CpM(CO)PR_3$ species.[22]

Finally, the complex $[(CpRh)_2(\mu\text{-CO})(\mu\text{-dppm})]$, which contains (diphenylphosphino)methane, carbonyl bridges, and a metal–metal bond, does not react with iodomethane. Iodine, however, reacts slowly to afford $Cp_2Rh_2(CO)(\mu\text{-dppm})I_2$ assumed by the authors to be a mixed-valence $Rh^{III}Rh^{I}$ compound in which some interaction of one of the iodide carried by the rhodium(III) center with the rhodium(I) center could explain the rather high stretching frequency observed for the CO group of this rhodium(I) site.[23] In addition, the cationic complex $[CpBr_2Rh(\mu\text{-dppm})Rh(CO)BrCp]Br_3$ was isolated from the reaction with bromine.

The present study concerns the recently prepared[1b,c] compound $[Rh(CO)(\mu\text{-}CpPPh_2)]_2$ (1), which combines characteristic features of the above cited complexes, namely 18-electron sites, a constrained double-bridged skeleton, and a long metal–metal distance. It was expected that its reactivity toward the usual electrophilic reagents would bring some new insights into the question of cooperativity of metal activation sites in coordination chemistry. Part of this study has been extended to the iridium analogue $[Ir(CO)(\mu\text{-}CpPPh_2)]_2$ (12) as starting material and is shortly described.

Experimental Section

General Remarks. All reactions and manipulations were routinely performed under nitrogen or argon atmosphere in Schlenk-type glassware. All solvents were appropriately dried and deoxygenated prior to use. Tetrahydrofuran (THF), diethyl ether, and toluene were purified before use by distillation from sodium benzophenone. Microanalyses were performed by the Service de Microanalyses du Laboratoire de Chimie de Coordination du CNRS. Mass spectra were recorded on a Varian MAT 311 A instrument. Infrared spectra of hexane or dichloromethane solutions were recorded using a Perkin-Elmer Model 225 grating spectrometer. The spectra were calibrated with water vapor lines in the carbonyl stretching region. ^1H NMR spectra were obtained at 90 MHz on a Bruker WH 90 FT instrument and/or at 250 MHz on a Bruker WM 250 FT spectrometer. Chemical shifts were referenced to internal tetramethylsilane. ^{13}C NMR spectra were obtained at 62.9 MHz on a Bruker WM 250 FT spectrometer (chemical shifts were also referenced to tetramethylsilane). ^{31}P NMR spectra were obtained at 36.4 MHz on a Bruker WH 90 FT spectrometer and/or at 101.1 MHz on a Bruker WM 250 FT spectrometer, and chemical shifts were referenced to external H_3PO_4.

Preparation of the Compounds. (Diphenylphosphino)cyclopentadiene[24] an ((diphenylphosphino)cyclopentadienyl)thallium[25] were prepared according to published procedures. The starting materials 1 and 2 were prepared from $Rh_2Cl_2(CO)_4$ and Vaska's complex, according to published procedures.[1b]

$[Rh(CO)(CpPPh_2)]_2^{2+}(A^-)_2$ (A^- = BF_4^- (2a), PF_6^- (2a′)). Oxidation with $Cp_2Fe^+BF_4^-$. To a mixture of 1 (760 mg, 1 mmol) and $Cp_2Fe^+BF_4^-$ (546 mg, 2 mmol) was added CH_2Cl_2 (20 mL), leading to a suspension of the two initial compounds that progressively disappeared, giving rise to a new red-orange precipitate. After stirring for an additional 1 h, the crystalline red-orange precipitate (**2a**) was isolated by filtration, washed with dichloromethane (3 × 10 mL), and dried under vacuum for 5 h (quantitative yield). Anal. Calcd for $Rh_2C_{36}H_{28}O_2P_2B_2F_8$: C, 46.25; H, 3.00. Found: C, 46.62; H, 3.46.

Oxidation with $Ag^+PF_6^-$. As above, CH_2Cl_2 (10 mL) was added to a mixture of 1 (380 mg, 0.5 mmol) and $Ag^+PF_6^-$ (253 mg, 1 mmol). The yellow color of the two initial products rapidly turned dirty yellow (the IR spectrum shows that this is an intermediate product) accompanied by the formation of a red-orange precipitate together with a silver mirror on the walls of the vessel. The liquid phase was eliminated after 3 h by filtration, and the solid residue was washed several times with dichloromethane until the washing solution became colorless. Acetone (20 mL) then was added to extract the oxidation product, **2a′**. From this solution, **2a′** was obtained in 60% yield. Anal. Calcd for $Rh_2C_{36}H_{28}O_2P_4F_{12}$: C, 42.62; H, 2.95. Found: C, 43.00; H, 3.21.

It should be noted that, depending on the nature of the counterion, the solubility differs: the salt **2a′** is highly soluble in polar solvants such as acetone and acetonitrile, while **2a** is soluble in acetonitrile but not in acetone.

$[Rh(py)(CpPPh_2)]_2^{2+}(BF_4^-)_2$ (2b). To $[Rh(CO)(CpPPh)_2]_2^{2+}(BF_4^-)_2$ (**2a**) (467 mg, 0.5 mmol) was added 10 mL of pyridine. The mixture progressively turned blue-green. The reaction was completed within 5 h. Pyridine was evaporated under vacuum and the solid residue, **2b**, was washed with diethyl ether and obtained in 72% yield. Anal. Calcd for $Rh_2C_{44}H_{38}N_2O_2P_2B_2F_8$: C, 51.00; H, 3.70; N, 2.70. Found: C, 51.32; H, 4.00; N, 2.77. Monocrystals of $[Rh(py)(CpPPh)_2]_2^{2+}(BF_4^-)_2$·MeOH suitable for an X-ray analysis were obtained by recrystallization at ambient temperature from a solution of **2b** in diethyl ether/methanol (Et_2O/MeOH, 1:4).

(16) (a) Beveridge, K. A.; Bushnell, G. W.; Dixon, K. R.; Eadie, D. T.; Stobart, S. R.; Atwood, J. L.; Zaworotko, M. J. *J. Am. Chem. Soc.* **1982**, *104*, 920. (b) Coleman, A. W.; Eadie, D. T.; Stobart, S. R.; Atwood, J. L.; Zaworotko, M. J. *J. Am. Chem. Soc.* **1982**, *104*, 922. (c) Beveridge, K. A.; Bushnell, G. W.; Stobart, S. R.; Atwood, J. L.; Zaworotko, M. J. *Organometallics* **1983**, *2*, 1447. (d) Beveridge, K. A.; Bushnell, G. W.; Dixon, K. R.; Eadie, D. T.; Stobart, S. R.; Atwood, J. L.; Zaworotoko, M. J. *Inorg. Chem.* **1984**, *23*, 4050. (e) Harrison, D. G.; Stobart, S. R. *J. Chem. Soc., Chem. Commun.* **1986**, 285.

(17) Schenck, T. G.; Milne, C. R. C.; Sawyer, J. F.; Bosnich, B. *Inorg. Chem.* **1985**, *24*, 2338.

(18) Scott, J. D.; Puddephatt, R. J. *Organometallics* **1986**, *5*, 2552.

(19) Ling, S. S. M.; Job, I. R.; Manojlovic-Muir, L.; Muir, K. W.; Puddephatt, R. J. *Organometallics* **1985**, *4*, 1198.

(20) Scholz, H. J.; Werner, H. *J. Organomet. Chem.* **1986**, *303*, C8.

(21) Faraone, F.; Bruno, G.; Tresoldi, G.; Faraone, G. *J. Chem. Soc., Dalton Trans.* **1981**, 1651.

(22) (a) Oliver, A. J.; Graham, W. A. G. *Inorg. Chem.* **1970**, *9*, 243. (b) Oliver, A. J.; Graham, W. A. G. *Inorg. Chem.* **1970**, *9*, 2653. (c) Hart-Davis, A. J.; Graham, W. A. G. *Inorg. Chem.* **1970**, *9*, 2658. (d) Oliver, A. J.; Graham, W. A. G. *Inorg. Chem.* **1971**, *10*, 1165. (e) Hart-Davis, A. J.; Graham, W. A. G. *Inorg. Chem.* **1971**, *10*, 1653.

(23) Faraone, F.; Bruno, G.; Schiavo, S. L.; Tresoldi, G.; Bombieri, G. *J. Chem. Soc., Dalton Trans.* **1983**, 433.

(24) Mathey, F.; Lampin, C. *Tetrahedron* **1975**, *31*, 2685.

(25) Raush, M. D.; Edwards, B. E.; Rogers, R. D.; Atwood, J. C. *J. Am. Chem. Soc.* **1983**, *105*, 3882.

$[Rh(CH_3CN)(CpPPh_2)]_2^{2+}(BF_4^-)_2$ (2c). The synthesis was carried out by decarbonylation of **2a** in acetonitrile. To a mixture of **2a** (467 mg, 0.5 mmol) and $Me_3NO{\cdot}2H_2O$ (112 mg, 1 mmol) was added acetonitrile (20 mL), and this was stirred for 10 min. A violet solution was formed. After further stirring for 20 min, the solvent was evaporated under vacuum. The resulting residue was redissolved in 10 mL of dichloromethane. The product was precipitated by addition of 5 mL of diethyl ether and subsequently filtrated and dried (yield 72%). Anal. Calcd for $Rh_2C_{38}H_{34}N_2P_2B_2F_8$: C, 47.50; H, 3.54; N, 2.92. Found: C, 47.90; H, 3.78; N, 3.04. Mass spectra (FD): m/e 352 for $[M^{2+} - 2CH_3CN]$.

$[Rh[P(OMe)_3](CpPPh)_2]_2^{2+}(BF_4^-)_2$ (2d). Decarbonylation of **2a** (470 mg, 0.5 mmol) by $Me_3NO{\cdot}2H_2O$ (113 mg, 1 mmol) in 10 mL of CH_2Cl_2 afforded a green solution, which was filtered. $P(OMe)_3$ (118 μL, 1 mmol) then was added. The initial green solution immediately turned red-purple. The product was precipitated by addition of 10 mL of ether and isolated by filtration and drying under vacuum for 10 h (yield 63%). Anal. Calcd for $Rh_2C_{40}H_{43}O_6P_4B_2F_8$: C, 42.66; H, 4.12. Found: C, 42.55; H, 4.27. The reaction may be carried out in acetone, THF, or benzene as well, affording similar yields.

$[Ir(CO)(CpPPh_2)]_2^{2+}(A^-)_2$ ($A^- = BF_4^-$ (13a), PF_6^- (13b)) were prepared as previously stated or the rhodium compounds, although the reaction of the silver salts with $[Ir(CO)(CpPPh)_2]_2$ is slower than in the case of 1. With $AgPF_6$ ($A^- = PF_6^-$), the yield was 54%. Anal. Calcd for $Ir_2C_{36}H_{28}O_2P_4F_{12}$: C, 35.18; H, 2.30. Found: C, 35.60; H, 2.53. With Cp_2FeBF_4 ($A^- = BF_4^-$), the yield was 83%. Anal. Calcd for $Ir_2C_{36}H_{28}O_2P_2B_2F_8$: C, 38.86; H, 2.54. Found: C, 39.30; H, 2.78.

$[Rh_2(CO)(COCH_3)(I)(CpPPh_2)_2]$ (3). From $[Rh(CO)(CpPPh_2)]_2$ (1). To a solution of 1 (76 mg, 0.1 mmol) in 20 mL of CH_2Cl_2 was added CH_3I (6.2 μL, 0.1 mmol) at room temperature. The mixture was stirred for 6 h. The initial orange solution darkened. The solution was concentrated to 3 mL, and diethyl ether (10 mL) was added, leading to precipitation of the product **3**, which was filtrated and washed with diethyl ether (2 × 5 mL) and recrystallized from a solution of toluene/CH_2Cl_2 (0.1:1 at −20 °C). **3** was obtained as red microcrystals in 87% yield. Anal. Calcd for $Rh_2C_{37}H_{31}O_2P_2I$: C, 49.25; H, 3.46; I, 14.06. Found: C, 49.52; H, 3.51; I, 13.84.

From $[Rh_2(CO)(COCH_3)(CpPPh_2)_2]^+PF_6^-$ (5a′). To a solution of **5a′** (92 mg, 0.1 mmol) in 5 mL of CH_2Cl_2 were added a few crystals of KI. The initial dark red solution immediately turned orange at room temperature. The reaction was complete within 30 min. The solvent was evaporated under vacuum. The residue was washed with methanol (2 × 2 mL), and the product was extracted from CH_2Cl_2 (5 mL). The solution was filtered. Addition of 10 mL of diethyl ether led to the formation of a precipitate, which was washed with 5 mL of ether and dried under vacuum for 3 h. **3** was obtained as a red microcrystalline product in nearly quantitative yield.

$[Rh(COCH_3)(I)(CpPPh_2)]_2$ (4). Methyl iodide (10 mL) was added to 1 (76 mg, 0.1 mmol) at room temperature. The mixture was stirred for 20 h. The excess of CH_3I was evaporated under vacuum. The residue was washed with diethyl ether (2 × 2 mL) and then dried under vacuum for 5 h. **4** was obtained as red microcrystals (96% yield). Anal. Calcd for $Rh_2C_{38}H_{34}O_2P_2I_2$: C, 43.71; H, 3.28; I, 24.31. Found: C, 43.98; H, 3.37; I, 24.01.

$[Rh_2(COCH_3)(CO)(CpPPh_2)_2]^+A^-$ ($A^- = CF_3SO_3^-$ (5a) or PF_6^- (5a′)). To a solution of 1 (125 mg, 0.2 mmol) in 100 mL of CH_2Cl_2 was added $CH_3SO_3CF_3$ (22 μL, 0.2 mmol) at 0 °C. The orange solution progressively turned dark red. After 1 h, the solvent was reduced to 5 mL under vacuum. Addition of 10 mL of ether led to precipitation of a red microcrystalline solid, which was filtered out, washed with diethyl ether (2 × 5 mL), and dried under vacuum (70% yield). Anal. Calcd for $Rh_2C_{38}H_{31}O_5P_2F_3S$: C, 49.37; H, 3.38. Found: C, 49.52; H, 3.51. The product **5a′** was obtained from a solution of **5a** dissolved in CH_2Cl_2 (2 mL) by precipitation with a saturated solution of $(n\text{-}Bu)_4NPF_6$ in MeOH (2 mL).

$[Rh(I)_2(CpPPh_2)]_2$ (7a). To a suspension of $[Rh(CO)(CpPPh_2)]_2$ (1) (152 mg, 0.2 mmol) in 10 mL of CH_2Cl_2 was added iodine (25.4 mg) in excess. After stirring for 30 min at room temperature, the initial orange suspension progressively turned maroon. The resulting precipitate was filtered off, washed with dichloromethane (2 × 5 mL), and then dried under vacuum (yield 96%). Anal. Calcd for $Rh_2C_{34}H_{28}P_2I_4$: C, 33.70; H, 2.33; I, 41.88. Found: C, 33.60; H, 2.51; I, 41.03. Mass spectra (IE): m/e 1085 (M^+ - I).

$[Rh_2(Cl)(CO)(CpPPh_2)_2]^+A^-$ (8b) and $[Rh_2Cl_2(CO)(CpPPh_2)_2]$ (6b). To a solution of 1 (152 mg, 0.2 mmol) in 50 mL of CH_2Cl_2 was added chlorine at room temperature with a syringe. The solution immediately turned green. A red-orange precipitate then formed gradually. After 30 min, the solvent was evaporated under vacuum and the residue was treated with 10 mL of CH_3OH. The orange-red precipitate then was separated by filtration from the green solution containing the monocationic product **8b**. A solution of methanol (10 mL) saturated with $(n\text{-}Bu)_4N^+PF_6^-$ then was added to the green solution. The salt **8b′** ($A^- = PF_6^-$) precipitated and was filtered off, washed with methanol (3 × 2 mL), and then dried under vacuum (57% yield). Anal. Calcd for $Rh_2C_{35}H_{28}OP_3ClF_6$: C, 46.6; H, 3.09; Cl, 3.88. Found: C, 45.82; H, 3.14; Cl, 3.40. Mass spectra (FD): m/e 769 (M^+) corresponding to the cationic part of the molecule. The red-orange precipitate **6b** was washed with dichloromethane (2 × 2 mL) and dried (31% yield). Anal. Calcd for $Rh_2C_{35}H_{28}OP_2Cl_2$: C, 52.33; H, 3.51; Cl, 8.83. Found: C, 52.62; H, 3.59; Cl, 8.41.

$[Rh(I)(CpPPh_2)]_2$ (9a). A suspension of **2a** (934 mg, 1 mmol) and Me_3NO (224 mg, 2 mmol) in 20 mL of CH_2Cl_2 was stirred for 20 min, affording a green solution. When allowed to react with KI (500 mg), this solution progressively turned red. After 2 h, its volume was reduced to 5 mL under vacuum and MeOH (10 mL) was added, leading to the precipitation of a microcrystalline product, **9a** (796 mg, 83% yield). Anal. Calcd for $Rh_2C_{34}H_{28}P_2I_2$: C, 42.62; H, 2.95; I, 26.49. Found: C, 42.93; H, 3.04; I, 26.20. Mass spectra: m/e 813 (M^+ − I).

$[Rh(Cl)(CpPPh_2)]_2$ (9b). The same method as for **9a** was used. **2a** (934 mg, 1 mmol) was decarbonylated by $Me_3NO{\cdot}2H_2O$ (224 mg, 2 mmol) in dichloromethane. The resulting green solution was stirred at room temperature with an excess of LiCl. The reaction was complete within 20 min. The solution then was filtrated and concentrated under vacuum to a volume of 5 mL. Addition of 10 mL of toluene was followed by precipitation of the dichloride as a red precipitate, which was washed with toluene (2 × 2 mL) and dried under vacuum for 10 h (yield 68%). Anal. Calcd for $Rh_2Cl_2C_{34}H_{28}P_2$: C, 52.68; H, 3.64; Cl, 9.15. Found: C, 53.01; H, 3.92; Cl, 9.01.

$[Rh(CH_3)(CpPPh_2)]_2$ (10a) and $[Rh_2(CH_3)(I)(CpPPh_2)_2]$ (11). To a suspension of $[Rh(I)(CpPPh_2)]_2$ (**9a**) (192 mg, 0.2 mmol) in 10 mL of toluene was added dropwise MeLi (380 μL, 0.6 mmol) in diethyl ether solution (1.6 M) at −70 °C. The temperature then was raised to ambient temperature, and the solution was stirred for 2 h. The initial red suspension progressively turned blue. The solution was filtered on a short column (3 cm high) of neutral alumina. The column was then washed with 100 mL of diethyl ether. The eluents were gathered, and the solvent was evaporated under vacuum. The dimethylated product, **10a**, was obtained as a violet blue solid in 81% yield. Anal. Calcd for $Rh_2C_{36}H_{34}P_2$: C, 58.88; H, 4.67. Found: C, 59.20; H, 4.80. The monomethyl product, $[Rh_2(CH_3)(I)(CpPPh_2)_2]$ (11), was eluted with dichloromethane by using an alumina column. The solvent then was evaporated under vacuum. **11** was obtained as a solid. Anal. Calcd for $Rh_2C_{35}H_{31}P_2I$: C, 49.67; H, 3.69; I, 15.00. Found: C, 49.85; H, 3.81; I, 14.82. Compound **11** is recrystallized in toluene as dark blue crystals of $[Rh_2(CH_3)I(CpPPh_2)_2]PhMe$.

$[Rh(Ph)(CpPPh_2)]_2$ (10b). Same method as above. To a suspension of **9a** (192 mg, 0.2 mmol) in 10 mL of toluene was added dropwise PhLi (300 μL, 0.6 mmol, 1.6 M) in solution in THF (2.0 M) at −70 °C. The complex **9b** was obtained as a blue product in 79% yield. Anal. Calcd for $Rh_2C_{46}H_{38}P_2$: C, 64.35; H, 4.46. Found: C, 64.65; H, 4.49.

X-ray Data Collection and Reduction

Crystal data and intensity collection data parameters for **2b**, **5a′**, and **11** are summarized in Table I. Diffraction experiments were performed at 20 °C on a Enraf-Nonius CAD4 diffractometer with graphite-monochromatized Mo Kα radiation. A least-squares fit of 25 reflections ($8° < \theta < 17°$) was used to obtain the final lattice parameters and the orientation matrices for **2b**, **5a′**, and **11**, respectively. The observed extinctions were consistent with the space group $P2_1/n$ for **2b**, $P2_12_12_1$, for **5a′**, and $P2_1/n$ for **11**. During data collection, of which the process is described else-

Table I. Summary of Crystal Data and Intensity Collection Parameters for $[Rh^{II}(\mu\text{-}CpPPh_2)(NC_5H_5)]^{2+}(BF_4^-)_2(MeOH)$ (2b), $[(CH_3CO)Rh^{II}(\mu\text{-}CpPPh_2)_2Rh^{II}(CO)]^+PF_6^-$ (5a'), and $[(Me_{0.93}I_{0.07})Rh^{II}(\mu\text{-}CpPPh_2)_2Rh^{II}(I)]PhMe$ (11)

	$B_2C_{45}F_8H_{42}N_2OP_2Rh_2$	$C_{37}F_6H_{31}O_2P_3Rh_2$	$C_{44.93}H_{38.79}I_{1.07}P_2Rh_2$
fw	1068.2	920.4	946.3
cryst color, form	brown parallelepiped	deep red plate	blue-dark parallelepiped
cryst syst	monoclinic	orthorhombic	monoclinic
space group	$P2_1/n$	$P2_12_12_1$	$P2_1/n$
a, Å	12.896 (2)	15.046 (2)	14.802 (2)
b, Å	23.262 (2)	17.209 (3)	15.894 (2)
c, Å	16.726 (2)	13.588 (2)	16.784 (3)
β, deg	107.12 (2)		104.35 (1)
V, Å^3	4795 (2)	3519 (2)	3825 (2)
d(calcd), g/cm^3	1.48	1.74	1.64
Z	4	4	4
cryst dimens, mm	0.35 × 0.35 × 0.25	0.35 × 0.10 × 0.125	0.35 × 0.20 × 0.15
abs coeff μ, cm^{-1}	8.1	11.2	18.1
(Mo Kα radiation), Å	0.710 73	0.710 73	0.710 73
scan mode	$\omega/2\theta$	$\omega/2\theta$	$\omega/2\theta$
scan range, deg	1.10 + 0.35 tan θ	1.00 + 0.35 tan θ	0.90 + 0.35 tan θ
scan rate, deg/min	1.1–8.2	1.1–8.2	1.1–8.2
no. of recorded data	7391	9342	6991
transm coeff		0.98–1.00	0.92–1.00
no. of unique data used	7046 ($0kl$ and $0k\bar{l}$ merged R_{av} = 0.027)	5886 (3456 $\bar{h}kl$ reflns meas for absolute configuration determination)	6725 ($0kl$ and $0k\bar{l}$ merged R_{av} = 0.018)
obs criterion	$F_o^2 \geq 2\sigma(F_o^2)$	$F_o^2 \geq 3\sigma(F_o^2)$	$F_o^2 \geq 3\sigma(F_o^2)$
no. of utilized data	4289	4581	4713

where[26] (3° < 2θ < 47°, +*h*,+*k*,±*l* data for **2b**; 3° < 2θ < 61°, +*h*,+*k*,+*l* data and 3° < 2θ < 50°, ±*h*,+*k*,+*l* data for **5a'**; 3° < 2θ < 50°, +*h*,+*k*,±*l* data for **11**), intensity data of three reflections were monitored every 2 h. For **2b**, these intensities linearly decreased about 15%; for **5a'** and **11** they showed only random, statistical fluctuations. The data were reduced in the usual way with the SDP[27] package, with linear decay corrections for **2b**. Empirical absorption corrections[28] were applied to data sets **5a'** and **11** on the basis of four ψ scans.

Structure Solution and Refinement

Non-hydrogen atomic scattering factors (f', f'') were taken from ref 29; hydrogen ones, from ref 30. In all cases, heavy-atom positions were determined by the Patterson method using the SHELXS-86 program.[31] The remaining non-hydrogen atoms were located from successive difference Fourier map calculations. Refinements were carried out with the SHELX-76 program[32] by using full-matrix least-squares techniques on F_o, minimizing the function $\sum w(|F_o| - |F_c|)^2$.

$[Rh^{II}(\mu\text{-}CpPPh_2)(NC_5H_5)]_2^{2+}(BF_4^-)_2(MeOH)$ (2b). Cp and Ph rings were refined as isotropic rigid groups (C–C = 1.420 and 1.395 Å, respectively). All other non-hydrogen atoms were refined anisotropically. H atoms, but those of the MeOH solvent which were omitted, were introduced in calculated positions (C–H = 0.97 Å) with a general isotropic temperature factor kept fixed to 0.065 Å^2. The refinement converged to R = 0.042 and R_w = 0.045 with a maximum shift/esd of 0.10 (a thermal parameter of the solvent molecule) on the final cycle (mean value 0.020) with 323 variable parameters. The best fit was S = 2.17 with unit weights. The maximum residual peak was near a F atom at 0.6 e/Å^3. Fractional atomic coordinates are given in Table II.

$[(CH_3CO)Rh^{II}(\mu\text{-}CpPPh_2)_2Rh^{II}(CO)]^+PF_6^-$ (5a'). Except Ph rings, which were refined as isotropic rigid groups (C–C = 1.395 Å), all non-H atoms were refined anisotropically. All H atoms were observed but introduced in calculations in constrained geometry (C–H = 0.97 Å) with general isotropic temperature factors, first refined and then kept fixed to 0.10 Å^2 for methyls and to 0.065 Å^2 for others. Both enantiomers were tested and the best one kept: R_{w_1} = 0.027, R_{w2} = 0.032 and by comparing $F_o(hkl)/F_o(\bar{h}kl)$ to $F_c(hkl)/F_c(\bar{h}kl)$ for 60 reflections in the same range of intensity.

The refinement converged to R = 0.027 and R_w = 0.027 with a maximum shift/esd of 0.008 on the final cycle with 283 variable parameters. A fit of S = 1.02 for the data using the weighting scheme $w = [\sigma^2(F_o) + 0.0003F_o^2]^{-1}$ was obtained. The maximum residual peak was near the Rh(2) atom at 0.6 e/Å^3. Fractional atomic coordinates are given in Table III.

$[(Me_{0.93}I_{0.07})Rh^{II}(\mu\text{-}CpPPh_2)_2Rh^{II}(I)]PhMe$ (11). Cp and Ph, including a disordered toluene molecule, were refined as isotropic rigid groups (C–C = 1.420 Å for Cp, 1.395 Å for Ph). Occupancy factors of methyl C(1) and I(1) atoms bonded to Rh(1) were first refined and then kept fixed to 0.93 and 0.07 respectively. C(1) and I(1) atoms were then refined isotropically. Similarly, occupancy factors of the disordered toluene molecule were refined and then kept fixed to 0.65 and 0.35. All other non-H atoms were refined anisotropically. H atoms of the C(1) methyl atom and of the disordered toluene molecule were not calculated. Other H atoms were introduced in constrained geometry (C–H = 0.97 Å) with a general isotropic temperature factor, first refined and then kept to 0.07 Å^2. The refinement converged to R = 0.045 and R_w = 0.048 with a maximum shift/esd of 0.081 (a thermal parameter of PhMe) on the final cycle (mean value 0.011) with 156 variable parameters. The best fit was S = 1.51 with the weighting scheme $w = [\sigma^2(F_o) + 0.0002F_o^2]^{-1}$. The maximum residual peak was on the disordered toluene molecule at 1 e/Å^3. Fractional atomic coordinates are given in Table IV.

Results and Discussion

The ordinary oxidative addition reactions of mononuclear compounds correspond per se to an increase of the formal oxidation number of the metal by two units.

Considering a priori the same type of reaction on the two metal atoms of a bimetallic system can naturally only increase their formal oxidation numbers by one unit per atom.[33] In other words, prior to study of the oxidative addition reactions themselves, it was desired to learn a little more about the accessible oxidation states of our bimetallic species.

(26) Mosset, A.; Bonnet, J. J.; Galy, J. *Acta Crystallogr., Sect. B* **1977**, *B33*, 2639.
(27) *SDP, Structure Determination Package*; Frenz, B. A. & Associates, Inc. and Enraf-Nonius: College Station, TX 77840, and Delft, Holland, 1985.
(28) North, A. C. T.; Phillips, D. C.; Mathews, F. S. *Acta Crystallogr., Sect. A* **1968**, *A24*, 351.
(29) *International Tables for X-ray Crystallography*; Ibers, J. A., Hamilton, W. C., Eds.; Kynoch Press: Birmingham, England, 1974; Vol. IV, Table 2.2.B, pp 99–101 and Table 2.3.1. pp 149–150.
(30) Stewart, R. F.; Davidson, E. R.; Simpson, W. T. *J. Chem. Phys.* **1965**, *42*, 3175.
(31) Sheldrick, G. M. *SHELXS-86, Program for Crystal Structure Solution*; University of Göttingen: Göttingen, Federal Republic of Germany, 1986.
(32) Sheldrick, G. M. *SHELX-76, Program for Crystal Structure Determination*; University of Cambridge: Cambridge, England, 1976.
(33) Poilblanc, R. *New J. Chem.* **1978**, *2*, 145.

Table II. Fractional Atomic Coordinates and Isotropic or Equivalent Temperature Factors[a] (Å² × 100) with Esd's in Parentheses for 2b

atom	x/a	y/b	z/c	U_{eq}/U_{iso}
Rh(1)	0.82428 (5)	0.18090 (3)	0.72964 (4)	4.2 (1)
Rh(2)	0.69503 (5)	0.0893 (3)	0.66713 (4)	4.3 (1)
P(1)	0.6569 (2)	0.21104 (9)	0.7301 (1)	4.5 (4)
P(2)	0.8352 (2)	0.04630 (9)	0.7647 (1)	4.4 (4)
N(1)	0.8155 (5)	0.2279 (3)	0.6172 (4)	4 (1)
N(2)	0.7652 (5)	0.0600 (3)	0.5723 (4)	6 (1)
C(1)	0.9127 (4)	0.1103 (2)	0.8034 (3)	3.5 (2)
C(2)	0.8868 (4)	0.1513 (2)	0.8574 (3)	5.4 (2)
C(3)	0.9446 (4)	0.2026 (2)	0.8533 (3)	4.8 (2)
C(4)	1.0062 (4)	0.1933 (2)	0.7967 (3)	5.6 (2)
C(5)	0.9865 (4)	0.1363 (2)	0.7659 (3)	5.0 (2)
C(6)	0.5794 (5)	0.1466 (2)	0.6956 (3)	5.0 (2)
C(7)	0.5372 (5)	0.1322 (2)	0.6096 (3)	5.9 (2)
C(8)	0.5149 (5)	0.0723 (2)	0.6040 (3)	6.2 (2)
C(9)	0.5434 (5)	0.0497 (2)	0.6864 (3)	7.0 (3)
C(10)	0.5832 (5)	0.0957 (2)	0.7431 (3)	6.0 (2)
C(11)	0.6464 (4)	0.2295 (3)	0.8309 (4)	6.4 (2)
C(12)	0.7209 (4)	0.2687 (3)	0.8788 (4)	6.8 (3)
C(13)	0.7074 (4)	0.2902 (3)	0.9529 (4)	7.4 (3)
C(14)	0.6193 (4)	0.2725 (3)	0.9791 (4)	7.6 (3)
C(15)	0.5447 (4)	0.2333 (3)	0.9312 (4)	8.5 (3)
C(16)	0.5583 (4)	0.2118 (3)	0.8571 (4)	8.1 (3)
C(17)	0.5818 (3)	0.2671 (2)	0.6643 (3)	4.8 (2)
C(18)	0.6331 (3)	0.3176 (2)	0.6515 (3)	6.4 (2)
C(19)	0.5715 (3)	0.3641 (2)	0.6108 (3)	6.7 (2)
C(20)	0.4586 (3)	0.3601 (2)	0.5829 (3)	6.7 (2)
C(21)	0.4073 (3)	0.3096 (2)	0.5957 (3)	7.1 (3)
C(22)	0.4689 (3)	0.2631 (2)	0.6364 (3)	7.0 (3)
C(23)	0.8010 (4)	0.0126 (2)	0.8528 (3)	5.2 (2)
C(24)	0.8648 (4)	0.0205 (2)	0.9353 (3)	6.8 (3)
C(25)	0.8342 (4)	−0.0046 (2)	1.0007 (3)	7.2 (3)
C(26)	0.7399 (4)	−0.376 (2)	0.9836 (3)	7.1 (3)
C(27)	0.6762 (4)	−0.0455 (2)	0.9011 (3)	6.9 (3)
C(28)	0.7067 (4)	−0.0204 (2)	0.8357 (3)	6.8 (3)
C(29)	0.9264 (4)	−0.0051 (2)	0.7386 (3)	4.4 (2)
C(30)	1.0390 (4)	−0.0001 (2)	0.7689 (3)	4.4 (2)
C(31)	1.1050 (4)	−0.0443 (2)	0.7554 (3)	6.6 (2)
C(32)	1.0584 (4)	−0.0934 (2)	0.7116 (3)	6.6 (2)
C(33)	0.9458 (4)	−0.0984 (2)	0.6813 (3)	6.4 (2)
C(34)	0.8798 (4)	−0.0542 (2)	0.6948 (3)	5.7 (2)
C(35)	0.7457 (6)	0.2113 (4)	0.5434 (5)	5 (2)
C(36)	0.7233 (7)	0.2477 (4)	0.4746 (5)	6 (2)
C(37)	0.7875 (7)	0.2950 (4)	0.4776 (5)	6 (2)
C(38)	0.8723 (6)	0.3067 (4)	0.5509 (5)	6 (2)
C(39)	0.8876 (6)	0.2692 (3)	0.6174 (5)	5 (2)
C(40)	0.8498 (6)	0.0891 (4)	0.5607 (5)	6 (2)
C(41)	0.8953 (7)	0.0737 (4)	0.4984 (5)	6 (2)
C(42)	0.8595 (7)	0.0233 (4)	0.4534 (5)	6 (2)
C(43)	0.7747 (7)	−0.0068 (4)	0.4676 (5)	7 (2)
C(44)	0.7254 (6)	0.0125 (4)	0.5261 (5)	5 (2)
B(1)	0.4688 (8)	0.1157 (5)	0.3648 (7)	6 (2)
F(1)	0.5019 (5)	0.1645 (3)	0.4116 (4)	9 (1)
F(2)	0.5473 (5)	0.0998 (3)	0.3301 (4)	10 (1)
F(3)	0.4519 (5)	0.0723 (3)	0.4133 (4)	10 (1)
F(4)	0.3756 (5)	0.1261 (3)	0.3040 (4)	9 (1)
B(2)	0.2706 (9)	0.1756 (5)	0.7590 (7)	6 (2)
F(5)	0.2389 (5)	0.1252 (3)	0.7841 (4)	10 (1)
F(6)	0.3111 (5)	0.1649 (3)	0.6904 (4)	11 (2)
F(7)	0.1868 (5)	0.2128 (3)	0.7367 (4)	11 (2)
F(8)	0.3493 (5)	0.2003 (3)	0.8253 (4)	10 (2)
O	0.3921 (6)	0.0996 (4)	0.8742 (5)	11 (2)
C(45)	0.433 (1)	0.0407 (6)	0.8803 (8)	11 (3)

[a] U_{eq} = one-third the trace of $\tilde{U}$.

Table III. Fractional Atomic Coordinates and Isotropic or Equivalent Temperature Factors[a] (Å² × 100) with Esd's in Parentheses for 5a'

atom	x/a	y/b	z/c	U_{eq}/U_{iso}
Rh(1)	0.45585 (3)	0.84534 (2)	0.22572 (3)	3.76 (6)
Rh(2)	0.60644 (3)	0.76024 (2)	0.25737 (3)	4.28 (7)
P(1)	0.4461 (1)	0.74952 (9)	0.11114 (9)	4.1 (2)
P(2)	0.5682 (1)	0.78523 (8)	0.4139 (1)	3.5 (2)
C(1)	0.5165 (5)	0.9133 (4)	0.1392 (5)	6 (1)
O(1)	0.5480 (4)	0.9574 (3)	0.0927 (4)	9 (1)
C(2)	0.6875 (4)	0.8525 (4)	0.2521 (4)	6 (1)
O(2)	0.6712 (4)	0.9108 (3)	0.2831 (4)	8 (1)
C(3)	0.7651 (5)	0.7463 (6)	0.1908 (7)	12 (2)
C(4)	0.4633 (4)	0.8319 (3)	0.3907 (3)	3.9 (9)
C(5)	0.3865 (4)	0.7958 (4)	0.3518 (4)	4 (1)
C(6)	0.3282 (4)	0.8521 (4)	0.3142 (4)	5 (1)
C(7)	0.3696 (5)	0.9219 (4)	0.3205 (4)	6 (1)
C(8)	0.4551 (5)	0.9133 (3)	0.3657 (4)	5 (1)
C(9)	0.5393 (5)	0.6908 (3)	0.1420 (4)	5 (1)
C(10)	0.6299 (4)	0.7082 (4)	0.1096 (5)	6 (1)
C(11)	0.6862 (4)	0.6697 (5)	0.1787 (6)	8 (2)
C(12)	0.6362 (5)	0.6327 (4)	0.2461 (6)	8 (1)
C(13)	0.5457 (5)	0.6425 (3)	0.2252 (5)	6 (1)
C(14)	0.4556 (3)	0.7732 (2)	−0.0183 (2)	4.9 (1)
C(15)	0.4213 (3)	0.8431 (2)	−0.0536 (2)	5.3 (2)
C(16)	0.4244 (3)	0.8597 (2)	−0.1540 (2)	5.6 (2)
C(27)	0.4618 (3)	0.8063 (2)	−0.2192 (2)	6.6 (2)
C(18)	0.4962 (3)	0.7363 (2)	−0.1839 (2)	6.3 (2)
C(19)	0.4930 (3)	0.7198 (2)	−0.9835 (2)	5.7 (2)
C(20)	0.3531 (3)	0.6843 (2)	0.1125 (3)	4.1 (1)
C(21)	0.2672 (3)	0.7128 (2)	0.1262 (3)	5.6 (2)
C(22)	0.1945 (3)	0.6628 (2)	0.1184 (3)	7.1 (2)
C(23)	0.2078 (3)	0.5844 (2)	0.0968 (3)	6.3 (2)
C(24)	0.2937 (3)	0.5560 (2)	0.0831 (3)	6.1 (2)
C(25)	0.3664 (3)	0.6059 (2)	0.0190 (3)	5.1 (2)
C(26)	0.5446 (2)	0.7028 (2)	0.4922 (3)	3.8 (2)
C(27)	0.4640 (2)	0.6938 (2)	0.5417 (3)	4.4 (1)
C(28)	0.4504 (2)	0.6295 (2)	0.6025 (3)	5.5 (2)
C(29)	0.5175 (2)	0.5742 (2)	0.6137 (3)	5.7 (2)
C(30)	0.5981 (2)	0.5832 (2)	0.5643 (3)	5.4 (2)
C(31)	0.6116 (2)	0.6475 (2)	0.5035 (3)	5.1 (1)
C(32)	0.6275 (2)	0.8482 (2)	0.4989 (3)	3.7 (1)
C(33)	0.5821 (2)	0.8953 (2)	0.5655 (3)	5.0 (2)
C(34)	0.6293 (2)	0.9396 (2)	0.6338 (3)	5.4 (2)
C(35)	0.7220 (2)	0.9366 (2)	0.6354 (3)	4.9 (2)
C(36)	0.7674 (2)	0.8895 (2)	0.5688 (3)	4.9 (2)
C(37)	0.7201 (2)	0.8452 (2)	0.5005 (3)	4.4 (1)
P(3)	0.6695 (1)	0.5186 (1)	0.8955 (1)	5.2 (3)
F(1)	0.6744 (4)	0.6059 (2)	0.8695 (4)	10 (1)
F(2)	0.6650 (4)	0.4311 (2)	0.9204 (4)	11 (1)
F(3)	0.7002 (4)	0.4982 (3)	0.7901 (4)	14 (2)
F(4)	0.6339 (6)	0.5386 (3)	0.9950 (5)	18 (2)
F(5)	0.7677 (4)	0.5199 (4)	0.9236 (6)	17 (2)
F(6)	0.5730 (3)	0.5140 (4)	0.8586 (5)	14 (2)

[a] U_{eq} = one-third the trace of $\tilde{U}$.

1. Synthesis of New Rhodium(II) Bimetallic Complexes. The organometallic chemistry of rhodium(II) and iridium(II) is still little documented.[34] Concerning the cyclopentadienyl derivatives, in contrast with the case of cobalt,[35] only a few examples of rhodium(II) compounds were isolated, as di- or trimetallic species, namely $[CpRh(CO)(PR_3)]_2^{2+}$ (R = Me, OMe),[36] μ-η^5:η'^5-$C_{10}H_8$-$[Rh(CO)(PPh_3)]_2^{2+}$,[37] and $\{[CpRh(CO)(PPh_3)]_2Ag\}^{2+}$.[38] The only Rh(II) monometallic species observed were the products of oxidation of Cp*Rh(CO)(L) (Cp* = C_5Me_5 or C_5Ph_5) (L = PPh_3, $AsPh_3$, $P(OPh)_3$) with the ferrocenium salt $[Cp_2Fe][PF_6]$ and were detected by EPR analysis at −196 °C.[39]

(34) (a) Hughes, R. P. *Comprehensive Organometallics Chemistry*; Wilkinson, G., Stone, F. G. A., Abel, E. W., Eds.; Pergamon: New York, 1982; Vol. 5, p 277. (b) Leigh, P. G. J.; Richards, R. L. *Comprehensive Organometallics Chemistry*; Wilkinson, G., Stone, F. G. A., Abel, E. W., Eds.; Pergamon: New York, 1982; Vol. 5, p 541.

(35) Felthouse, T. R. *Prog. Inorg. Chem.* **1982**, *29*, 73.

(36) Fonseca, E.; Geiger, W. E.; Bitterwolf, T. E.; Rheingold, A. C. *Organometallics*, **1988**, *7*, 567.

(37) (a) McKinney, R. J. *J. Chem. Soc., Chem. Commun.* **1980**, 603. (b) Connely, N. J.; Lucy, A. R.; Payne, J. D.; Galas, A. M. R.; Geiger, W. E. *J. Chem. Soc., Dalton Trans.* **1985**, 973. (c) Freeman, M. J.; Orpen, A. G.; Connely, N. G.; Manner, I.; Raven, S. J. *J. Chem. Soc., Dalton Trans.* **1985**, 2283.

(38) Connely, N. G.; Lucy, A. R.; Galas, A. M. R. *J. Chem. Soc., Chem. Commun.* **1981**, 43.

Table IV. Fractional Atomic Coordinates and Isotropic or Equivalent Temperature Factors[a] (Å² × 100) with Esd's in Parentheses for 11

atom	x/a	y/b	z/c	U_{eq}/U_{iso}
Rh(1)	0.18641 (4)	0.79288 (3)	0.26734 (3)	3.60 (9)
Rh(2)	0.10518 (4)	0.92207 (4)	0.16957 (3)	3.8 (1)
C(1)[b]	0.2534 (7)	0.7426 (6)	0.1809 (6)	5.4 (3)
I(1)[b]	0.2611 (7)	0.7308 (6)	0.1448 (6)	6.3 (3)
I(2)	0.03289 (4)	0.82721 (4)	0.03855 (3)	6.0 (1)
P(1)	0.2988 (1)	0.8876 (1)	0.2955 (1)	3.7 (3)
P(2)	−0.0058 (1)	0.8812 (1)	0.2313 (1)	4.4 (4)
C(2)	0.0440 (4)	0.7884 (3)	0.2871 (3)	4.4 (2)
C(3)	0.0607 (4)	0.7126 (3)	0.2483 (3)	4.6 (2)
C(4)	0.1341 (4)	0.6689 (3)	0.3032 (3)	5.4 (2)
C(5)	0.1629 (4)	0.7178 (3)	0.3759 (3)	5.7 (2)
C(6)	0.1072 (4)	0.7916 (3)	0.3660 (3)	5.0 (2)
C(7)	0.2455 (4)	0.9690 (3)	0.2238 (3)	4.0 (2)
C(8)	0.1814 (4)	1.0278 (3)	0.2424 (3)	5.1 (2)
C(9)	0.1292 (4)	1.0638 (3)	0.1671 (3)	5.5 (2)
C(10)	0.1611 (4)	1.0256 (3)	0.1021 (3)	5.9 (2)
C(11)	0.2329 (4)	0.9677 (3)	0.1372 (3)	5.1 (2)
C(12)	0.4139 (4)	0.8638 (3)	0.2813 (3)	4.3 (2)
C(13)	0.4560 (4)	0.9054 (3)	0.2267 (3)	6.5 (3)
C(14)	0.5457 (4)	0.8830 (3)	0.2224 (3)	8.4 (3)
C(15)	0.5934 (4)	0.8190 (3)	0.2725 (3)	7.9 (3)
C(16)	0.5513 (4)	0.7774 (3)	0.3270 (3)	7.3 (3)
C(17)	0.4615 (4)	0.7998 (3)	0.3314 (3)	5.7 (2)
C(18)	0.3288 (4)	0.9389 (3)	0.3957 (3)	4.1 (2)
C(19)	0.3601 (4)	1.0220 (3)	0.4037 (3)	5.7 (2)
C(20)	0.3873 (4)	1.0589 (3)	0.4814 (3)	7.2 (3)
C(21)	0.3832 (4)	1.0127 (3)	0.5511 (3)	7.3 (3)
C(22)	0.3519 (4)	0.9296 (3)	0.5431 (3)	7.4 (3)
C(23)	0.3247 (4)	0.8927 (3)	0.4654 (3)	6.0 (2)
C(24)	−0.1215 (4)	0.8517 (3)	0.1731 (3)	5.3 (2)
C(25)	−0.1636 (4)	0.7764 (3)	0.1868 (3)	6.8 (3)
C(26)	−0.2551 (4)	0.7591 (3)	0.1437 (3)	8.2 (3)
C(27)	−0.3044 (4)	0.8171 (3)	0.0869 (3)	7.8 (3)
C(28)	−0.2622 (4)	0.8924 (3)	0.0732 (3)	8.0 (3)
C(29)	−0.1708 (4)	0.9097 (3)	0.1163 (3)	6.8 (3)
C(30)	−0.0376 (4)	0.9477 (4)	0.3084 (4)	5.5 (2)
C(31)	−0.0216 (4)	1.0341 (4)	0.3073 (4)	7.4 (3)
C(32)	−0.0517 (4)	1.0868 (4)	0.3620 (4)	9.5 (4)
C(33)	−0.0977 (4)	1.0531 (4)	0.4178 (4)	9.7 (4)
C(34)	−0.1137 (4)	0.9667 (4)	0.4189 (4)	10.3 (4)
C(35)	−0.0836 (4)	0.9140 (4)	0.3642 (4)	7.8 (3)
C(36)[c]	0.370 (1)	0.819 (1)	0.9504 (9)	13.1 (8)
C(37)[c]	0.275 (1)	0.837 (1)	0.9287 (9)	11.9 (7)
C(38)[c]	0.238 (1)	0.888 (1)	0.8610 (9)	13.1 (9)
C(39)[c]	0.296 (1)	0.921 (1)	0.8150 (9)	14.5 (9)
C(40)[c]	0.391 (1)	0.903 (1)	0.8368 (9)	12.7 (8)
C(41)[c]	0.428 (1)	0.851 (1)	0.9044 (9)	12.6 (8)
C(42)[c]	0.406 (2)	0.759 (2)	1.023 (1)	19 (1)
C(36)′[c]	0.329 (2)	0.900 (2)	0.852 (1)	9 (1)
C(37)′[c]	0.262 (2)	0.862 (2)	0.886 (1)	9 (1)
C(38)′[c]	0.289 (2)	0.819 (2)	0.961 (1)	8 (1)
C(39)′[c]	0.384 (2)	0.814 (2)	1.002 (1)	16 (2)
C(40)′[c]	0.450 (2)	0.852 (2)	0.968 (1)	21 (3)
C(41)′[c]	0.423 (2)	0.895 (2)	0.893 (1)	12 (1)
C(42)′[c]	0.296 (2)	0.941 (2)	0.767 (2)	11 (1)

[a] U_{eq} = one-third the trace of $\tilde{U}$. [b] C(1) and I(1) have occupancy factors of 0.93 and 0.07, respectively. [c] Disordered PhMe groups have occupancy factors of 0.65 and 0.35 respectively.

The oxidation of the dimetallic complexes **1** and **12** was easily performed by using stoichiometric amounts of ferrocenium tetrafluoroborate or silver or silver hexafluorophosphate as oxidant. In all cases the reactant and the oxidant were stirred in CH_2Cl_2 until a precipitate of the oxidized spcies was quantitatively obtained. The reactions with the ferrocenium salt were rapid and afforded the orange-red rhodium cationic spcies $[Rh(CO)(\mu\text{-}CpPPh_2)]_2^{2+}(BF_4^-)_2$ (**2a**) or the yellow iridium one $[Ir(CO)(\mu\text{-}CpPPh_2)]_2^{+}(BF_4^-)_2$ (**13**). The reactions with the silver salts were more complicated. In this case the dicationic species were produced slowly although the reactants **1** and **12** were consumed rapidly. An intermediate was formed, which was identified by a CO stretching vibration of different frequency from that of both the reactant and the product. The low solubility and low stability of this intermediate have limited our study of it. Nevertheless the fact that, when dissolved in acetone, it affords **1** (or **12**) and **2a** (or **13**) through a dismutation reaction, together with formation of a silver mirror, prompted us to propose the formulation: $\{[M(CO)(\mu\text{-}CpPPh_2)]_2Ag\}^+PF_6^-$ corresponding to the addition of 1 equiv of Ag^+ to the bimetallic complexes.

It is worthwhile noting here, that in contrast with the case of mononuclear species $CpM(CO)_2$, the dimetallic complexes **1** and **12** did not react with nucleophiles such as PPh_3 or CO under either thermal or photolytic conditions. As proposed by Rausch, Atwood et al.,[40] the failure of these reactions probably shows that the rigidity of the bridging frame prevents the η^5 to η^3 ring slippage postulated by Basolo[41] as a determining step for the substitution reactions on cyclopentadienylrhodium dicarbonyl complexes. Concerning the dicationic species **2a** and **13**, it was expected that the increase of the oxidation state would weaken the bonding strength of the remaining CO groups. Actually, the two CO groups in **2a** were easily replaced by pyridine, giving quantitatively $[Rh^{II}(py)(\mu\text{-}CpPPh_2)]_2^{2+}(BF_4^-)_2$ (**2b**), while weaker donor ligands such as the solvents acetonitrile, THF, acetone, or dichloromethane afforded no such reaction. In fact the nucleophilic attacks of pyridine on **2a**—an 18-electron compound, the metal–metal bonding pair being included—is still puzzling. Accepting that the rigidity of the bridging frame could prevent the slippage, we proposed further on a rationalization based on metal–metal bond breaking.

For comparison purposes, the reactions of the two series of complexes with the trimethylaminoxide were also studied. The oxidation of the carbonyl ligands in **1** and **12** was not observed, but as expected, in **2a** and **13** it appeared to be activated by the overall positive charge. This led to ready nucleophilic attack of the oxidant, and the carbonyl ligands were thus eliminated offering new synthetic potentialities. The reaction was performed in various solvents. In pyridine or acetonitrile the compounds **2b** and **2c** were respectively obtained. Also, in dichloromethane, acetone, THF, and even in *benzene*, the reaction led to green products either as solids or as solutions, depending on the solvent. The corresponding ^{31}P spectra showed that they were a mixture of several species which were not separated. Water introduced with the trimethylaminoxide can also act as ligand and is probably involved in some of these species.

Nevertheless such a mixture was currently used as starting material for synthesis; for instance it was transformed quantitatively into **2b** or into $[Rh[P(OMe)_3](\mu\text{-}CpPPh_2)]_2^{2+}(A^-)_2$, **2d** ($A^- = BF_4^-$ or PF_6^- depending on the starting salt).

Finally, it is noticeable that under our reaction conditions (see Experimental Section) we were unable to observe any photochemical reaction of **1** or **2a** in acetonitrile solution.

Spectroscopic Studies of the Dicationic Species $[M^{II}(L)(\mu\text{-}CpPPh_2)]_2^{2+}$ (2a–d, 13). The spectroscopic

(39) Connely, N. G.; Freeman, M. J.; Orpen, A. G.; Manners, I. *J. Chem. Soc., Dalton Trans.* **1984**, 2703.

(40) Rausch, M. D.; Spink, W. C.; Atwood, J. L.; Baskar, A. J.; Bott, S. G. *Organometallics* **1989**, *8*, 2627.

(41) (a) Schuster-Woldan, H. G.; Basolo, F. J. *J. Am. Chem. Soc.* **1966**, *88*, 1657. (b) Rerek, M. E.; Basolo, F. J. *Organometallics* **1983**, *2*, 372. (c) Rerek, M. E.; Basolo, F. J. *J. Am. Chem. Soc.* **1984**, *106*, 5908.

Table V. $^{31}P\{^1H\}$ and ^1H NMR Data for the Bimetallic Dicationic Rhodium(II) and Iridium(II) Compounds

compd[a]	$\delta(^{31}P)$, ppm in CD_3CN/CH_3CN	J_{P-Rh}, Hz	$\delta(^1H)$, ppm[b] in CD_3CN
$[Rh(CO)(CpPPh_2)]_2^{2+}(A^-)_2$ (2a)	43.2(AA'XX')	123	7.23, 6.15, 4.34 (8 H of Cp)
$[Rh(py)(CpPPh_2)]_2^{2+}(A^-)_2$ (2b)	44.2(AA'XX')	45.6	6.8 and 2.7 (8 H of Cp)
$[Rh(CH_3CN)(CpPPh_2)]_2^{2+}(A^-)_2$ (2c)	49.4(AA'XX')	148.5	7.31, 6.83, 5.98, 3.02 (8 H of Cp), 1.90 (s, 6 H of CH_3CN)
$[RhP(OMe)_3(CpPPh_2)]_2^{2+}(A^-)_2$ (2d)	129.6 (ddd)[d]	248.5	5.92 and 5.74 (8 H of Cp), 3.60 (d, J_{H-P} = 12.03 Hz, 18 H of CH_3)
	40.3 (ddd)[e]	129.7	
$[Ir(CO)(CpPPh_2)]_2^{2+}(A^-)_2$ (13)	3.4 (s)		7.40, 6.19, 4.65 (8 H of Cp)

[a] A = BF_4^-. [b] Except for the phenyl protons. [c] In $CDCl_3/CHCl_3$. [d] For $P(OMe)_3$. [e] For $-PPh_2$. [f] $J_{P(1)-P(2)}$ = 76.5, $J_{P-P(2)}$ = 7.3 Hz.

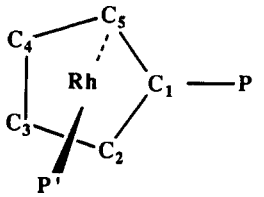

Figure 3. Trans disposition of the phosphorus P′ and carbon C_5 atoms on both sides of each of the rhodium centers.

data relative to the compounds **2a–d** and **13** are given in Tables V and VI. The $^{31}P\{^1H\}$ spectra of **2a–c** show significant second-order splitting patterns AA′XX′ with apparent coupling constants J_{P-Rh} that are weaker than in **1** (J_{P-Rh} = 200 Hz). For **13**, a singlet is observed at lower field than **12**. The $^{31}P\{^1H\}$ spectra of **2e** also contained the signal of the phosphite ligand. These observations are consistent with two equivalent metal centers.

In the ^1H and ^{13}C NMR spectra, the dicationic **2a** and **13** show respectively three and five different signals for the hydrogen and carbon atoms of the cyclopentadienyl groups. This is interpreted by the absence of any plane of symmetry perpendicular to the C_5H_4 planes and including the metal atoms. Such a situation is in contrast with previous observations[1a] concerning **1** and **12**. In these compounds, the apparent equivalence by a pair of the hydrogen and carbon atoms was assigned to a rapid interconversion process between two transoid forms. For **2c**, only two ^1H multiplets were clearly observed, the others being hidden by the aromatic protons of the pyridine ligands and phenyl groups but the ^{13}C spectra actually show five peaks associated with the ten carbon atoms of the two cyclopentadienyl ligands. Finally, the most significant ^1H NMR spectra were observed in **2d**: in this case all the four peaks corresponding to the eight protons of the two cyclopentadienyl ligands were clearly observed. One can also notice that the values of the proton chemical shifts are stretched over a large "field"(3–7 ppm for **2d**); this is interpreted as an indication of quite different environments on each side of the cyclopentadienyl group. Finally, we have observed in **2a**, **2c**, and **13** the existence of a triplet for one of the carbon atoms, leading us to consider its couplings with both phosphorus atoms, namely coupling inside the cyclopentadienyl phosphine ($J_{C(5)-P}$) or coupling through the metal ($J_{C(5)-P'}$) as shown in Figure 3.

Actually, the rigid conformation of the molecule (see also Figure 10) allows the carbon C_5 to be approximately in a trans position with respect to P′, which explains the coupling. Also, the couplings $J_{C(1)-P}$, $J_{C(2)-P}$ and $J_{C(2)-Rh}$ were observed but the non-zero value of $J_{C(2)-Rh}$ is not explained.

The crystal structure of **2b** shown on Figure 10 is in complete agreement with the above NMR data and is considered to be characteristic of all the dicationic species **2a–e** and **13**. In addition, the infrared spectra of **2a** shows two C–O stretching bands at 2086 and 2054 cm^{-1} (these two bands were not resolved in suspension in KBr[1c]), which, considering the cisoid position of the two C–O

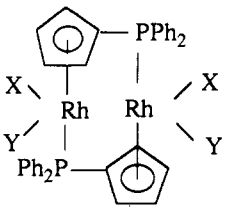

4 X = Y = I
7a X = I, Y = $COCH_3$

Figure 4. $[Rh^{III}]_2$ bimetallic complexes.

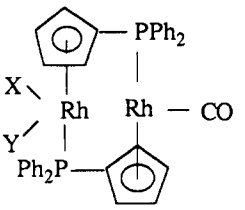

3 X = I, Y = $COCH_3$
6a X = Y = I
6b X = Y = Cl
6c X = I, Y = Cl

Figure 5. Mixed-valence Rh^{III},Rh^{I} bimetallic complexes.

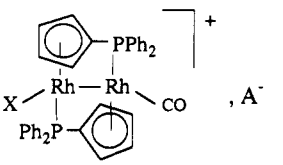

5a	X = $COCH_3$	A^- = $CF_3SO_3^-$
5a′	X = $COCH_3$	A^- = PF_6^-
8b	X = Cl	A^- = Cl^-
8b′	X = Cl	A^- = PF_6^-

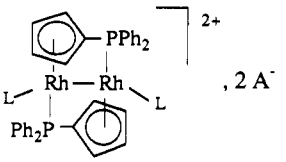

2a	L= CO	A^- = BF_4^-
2a′	L= CO	A^- = PF_6^-
2b	L= py	A^- = BF_4^-
2c	L = CH_3CN	A^- = BF_4^-
2d	L = $P(OMe)_3$	A^- = BF_4^-

Figure 6. Rh^{II}–Rh^{II} metal–metal-bonded cationic species.

groups, were attributed to the two expected stretching modes. Finally, the shift toward high frequencies observed in **2a** as compared with **1** is expected due to the oxidation states.

2. Reactions of the Homobimetallic $[Rh(CO)(\mu\text{-}CpPPh_2)]_2$ Compound 1 with Electrophiles. The reactions of iodomethane, methyl triflate, iodine, and chlorine with $[Rh(CO)(CpPPh_2)]_2$ (**1**) have been studied.

It has been reported[40] that no reaction takes place between complex **1** and iodomethane: in fact, the reaction is slow and needs a room-temperature period of over 20 h to allow its completion. The IR and NMR data are given in Tables VII and VIII. Under these conditions and with a ratio of CH_3I:Rh ≥ 1, a red product, **4**, analyzing for $[RhI(CH_3CO)(CpPPh_2)]_2$ was quantitatively obtained. It possesses an infrared band at 1675 cm^{-1} characteristic of an acetyl group and, in its $^{31}P\{^1H\}$ spectrum, and AA′XX′ signal centered at 31.5 ppm ($^1J_{Rh-P}$ = 170 Hz) in accordance with two identical metal centers each carrying one acetyl group and one iodide. Complex **4** (Figure 4) is

Table VI. $^{13}C\{^1H\}$ NMR Data for the Cyclopentadienyl and Other Groups in the Bimetallic Dicationic Rhodium(II) and Iridium(II) Compounds

compd	$\delta(C_1)$, ppm (J_{P-C}, Hz)	$\delta(C_2)$, ppm (J_{P-C}, Hz)	$\delta(C_5)$, ppm (J_{P-C}, Hz)	$\delta(C_4)$, ppm/$\delta(C_3)$, ppm[b]	other groups
$[Rh(CO)(CpPPh_2)]_2^{2+}(PF_6^-)_2$[a] (2a)	66.43 (d) (51.4)	88.76 (d) (12.0)	93.55 (dd) (10.7)	105.50 (s)/109.70 (s)	180.07 (dd) for CO (J_{PC} = 16.1, J_{RhC} = 75.9 Hz)
$[Rh(py)(CpPPh_2)]_2^{2+}(BF_4^-)_2$[a] (2b)	59.55 (d) (59.4)	68.44 (dd) (14.2/22.0)	95.75 (dd) (11.1)	98.75 (s)/115.27 (s)	
$[RhP(OMe)_3(CpPPh_2)]_2^{2+}(BF_4^-)_2$ (2d)	55.10 (d) (60.0)	88.04 (m)	91.73 (m)	98.86 (s)/101.98 (s)	54.55 (d) for Me (J_{PC} = 8.2 Hz)
$[Ir(CO)(CpPPh_2)]_2^{2+}(PF_6^-)_2$[a] (13)	67.71 (d) (59.4)	84.92 (d) (13.2)	87.90 (dd) (10.1)	101.01 (s)/103.81 (s)	163.00 (d) for CO (J_{PC} = 12.4 Hz)

[a] In $(CD_3)_2CO$. [b] CD_2Cl_2.

Table VII. C–O Stretching Frequencies of the Complexes Prepared by Oxidative Addition Reaction as with $[Rh(CO)(CpPPh_2)]_2$ (1)

compd	ν(CO), cm^{-1} (CH_2Cl_2)
$[Rh_2(CO)(COCH_3)(I)(CpPPh_2)_2]$ (3)	1962 (s), 167 (m)
$[Rh(COCH_3)(I)(CpPPh_2)]_2$ (4)	1675[a]
$[Rh_2(CO)(COCH_3)(CpPPh_2)_2]^+A^-$ (5)[b]	2025 (s), 1640 (m)[a]
$[Rh_2(CO)(I)_2(CpPPh_2)_2]$ (6a)	1960
$[Rh_2(CO)(Cl)_2(CpPPh_2)_2]$ (6b)	1970[a]
$[Rh_2(CO)(Cl)(I)(CpPPh_2)_2]$ (6c)	1963
$[Rh_2(CO)(Cl)(CpPPh_2)_2]^+A^-$ (8)[c]	2056

[a] Nujol. [b] $A^- = SO_3CF_3^-, PF_6^-$. [c] $A^- = Cl^-, PF_6^-$.

therefore the result of oxidative additions on each metal atom, followed by methyl migration. When a ratio of CH_3I:Rh = 1:2 was used (in solution in CH_2Cl_2), the disappearance of 1 was observed by infrared spectroscopy simultaneously with the appearance of two new bands at 1962 and 1676 cm^{-1}, respectively. The first one was assigned to a terminal carbonyl ligand on a rhodium(I) center, while the second band was attributed to a coordinated acetyl group. The corresponding product, **3**, was obtained as red crystals, analyzing as $Rh_2(CO)(I)(CH_3CO)(CpPPh_2)_2$. All the data allow us to propose for **3** a mixed-valence structure Rh(III)–Rh(I) in which the slight increase of the terminal C–O stretching frequencies (Table VII), compared to 1, precludes any significant direct interaction between the two metal centers (Figure 5).

The $^{31}P\{^1H\}$ spectrum (Table VIII) shows two doublets of doublets, respectively centered at 39.3 and 32.5 ppm, due to nonequivalent and mutually coupled phosphorus nuclei. The two different coupling values are attributed to the different oxidation states of the rhodium centers, namely $J_{P-Rh(I)}$ = 202.2 Hz, quite close to the value observed in 1, and $J_{P-Rh(III)}$ = 178.8 Hz close to that observed in **4**.

With the purpose of obtaining more informations about the pathway to **3** and **4**, the reaction of 1 with the carbocation CH_3^+ has been explored by using methyl triflate. The reaction of 1 with this reagent was performed in CH_2Cl_2 at −20 °C and yielded, after 6 h, a red product, a 1:1 electrolyte, analyzing as $[Rh_2(COCH_3)(CO)(CpPPh_2)_2]SO_3CF_3$ (**5a**). Red crystals of the hexafluorophosphate salt, **5a′** were easily obtained from a solution of **5a** in CH_2Cl_2 through precipitation with a saturated methanolic solution of $(n\text{-}Bu)_4NPF_6$.

The infrared spectrum of both monocationic species shows two bands, viz. at 2025 cm^{-1} for the C–O stretching mode and at 1640 cm^{-1}, characteristic of the acetyl group (Table VII).

The $^{31}P\{^1H\}$ NMR spectrum indicates that the two phosphorus atoms are nonequivalent. They appear as doublets of doublets and the two $^1J_{P-Rh}$ coupling constants, close to each other (167.7 and 144.1 Hz, respectively) argue clearly for a well-shared distribution of the positive charge. From these spectroscopic data, a structure containing a rhodium(II)–rhodium(II) bond was proposed (Figure 6): it has been confirmed by the X-ray diffraction study of **5a′** (vide infra).

Compound **5a** or **5a′** was rapidly transformed into **3** by the nucleophilic attack of iodide added as KI. Our observations on the reactions of 1 with iodomethane and with the carbocation CH_3^+ are summed up in Figure 7.

Iodine (molar ratio I_2:Rh = 1) reacted instantaneously with 1, leading to a brown precipitate analyzing as $Rh(I)_2(CpPPh_2)$ and the mass spectrum (EI) showed a peak (m/e = 1085) corresponding to $Rh_2I_3(CpPPh_2)_2$, readily explained by the loss of one iodine from the dinuclear

Table VIII. $^{31}P\{^1H\}$ and ^1H NMR Spectra[a] of the Complexes Prepared by Oxidative Addition Reactions with $[Rh(CO)(CpPPH_2)]_2$ (1)

complex	$\delta(^{31}P)$, ppm	J_{P-Rh}, Hz	$^3J_{P-Rh'}$, Hz	$J_{P-P'}$, Hz	$\delta(^1H)$, ppm[b]
$[Rh_2(CO)(COCH_3)(I)(CpPPh_2)_2]$ (3)	39.3 (dd)	200.2 (Rh^I)			6.2, 5.9, 4.1, 4.0 (four massifs, 8 H of 2 Cp), 2.9 (s large, 3 H of Me)
	32.5 (dd)	172.8 (Rh^{III})			
$[Rh_2(COCH_3)(I)(CpPPh_2)]_2$ (4)	31.5 (AA′XX′)	170.0 (Rh^{III})			6.6, 5.9, 5.7, 5.2 (four massifs, 8 H of 2 Cp), 2.8 (s large, 6 H of 2 Me)
$[Rh_2(CO)(COCH_3)(CpPPh_2)_2]^+A^-$ (5)[c]	47.6 (ddd)	167.7	4.4	4.4	large massif at 6.2–5.6 ppm (8 H of 2 Cp), 2.7 (s, large, 3 H of Me)
	39.4 (ddd)	144.1	4.4		
$[Rh_2(CO)(I)_2(CpPPh_2)_2]$ (6a)	45.3 (dd)	203.0 (Rh^I)		10.3	6.3, 6.2, 6.1, 5.9 (four massifs, 8 H of 2 Cp)
	18.0 (dd)	142.6 (Rh^{III})			
$[Rh_2(CO)(Cl)(I)(CpPPh_2)_2]$ (6c)	45.5 (dd)	202.9 (Rh^I)		10.3	
	18.7 (dd)	139.7 (Rh^{III}0			
$[Rh_2(CO)(Cl)(CpPPh_2)_2]^+PF_6^-$ (8b)	40.0 (ddd)	144.1	7.2	4.5	6.4, 5.5, 4.4, 3.8 (four massifs, 8 H of 2 Cp)
	38.2 (ddd)	146.1	4.5		

[a] In $CDCl_3$ or in $CDCl_3/CHCl_3$. [b] The protons of the phenyl groups are not considered. [c] $A^- = SO_3CF_3^-, PF_6^-$.

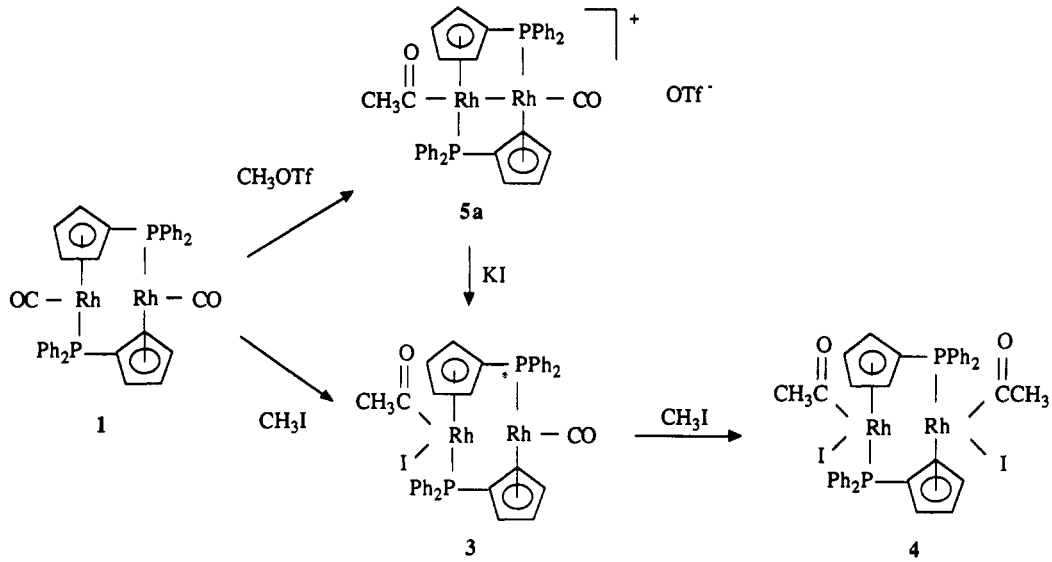

Figure 7. Oxidative addition of a methyl carbocation or methyl iodide on the dinuclear complex 1.

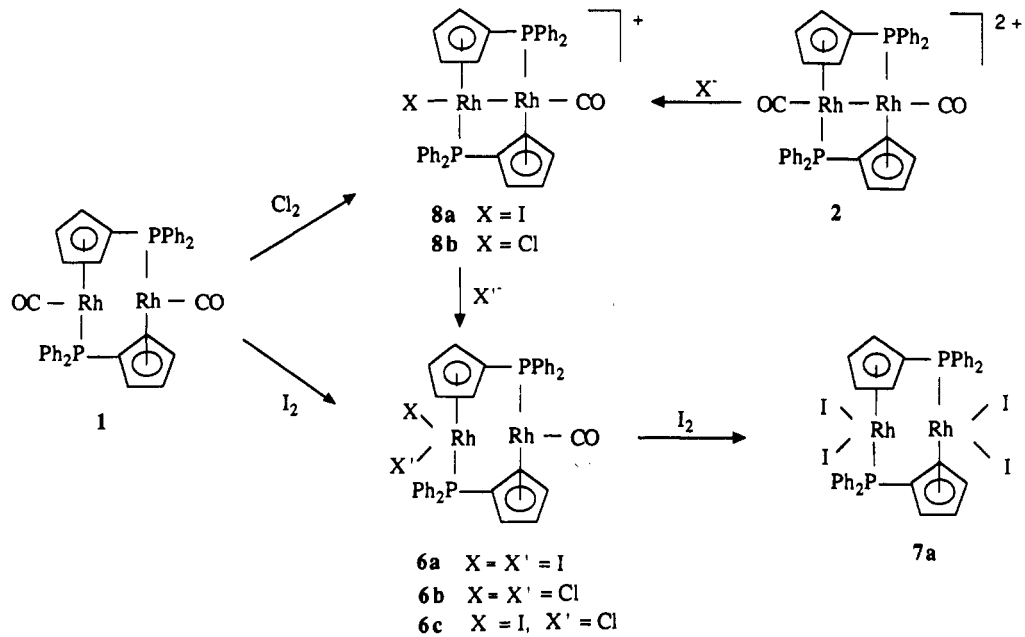

Figure 8. Oxidative addition of halogens on the dinuclear complex 1.

species $[Rh(I)_2(CpPPh_2)]_2$ (**7a**). Therefore the overall reaction is described as a double oxidative addition, apparently a mere duplication of the process observed with mononuclear compounds,[39] and quite symmetrical structure is proposed for **7a** (Figure 7).

For the ratio I_2:Rh = 1:2, the precipitation of **7a** was still observed but also the presence of a compound of (single) addition to only one metal center, **6a**, together with the unreacted starting material 1. Compound **6a** was characterized by NMR and infrared data (Tables VII and VIII). The $^{31}P\{^1H\}$ spectrum consists of two doublets of doublets corresponding to two nonequivalent coupled phosphorus atoms with very different J_{P-Rh} coupling constants. One of them, $J_{P(1)-Rh(1)}$ = 203.0 Hz, is very similar to the value measured in 1 but the other, i.e., $J_{P(2)-Rh(2)}$ = 142.6 Hz is quite different. These observations led to the proposal of two different oxidation states for the rhodium atoms, namely 1+ for Rh(1) and 3+ for Rh(2). In addition, the very small shift of the C–O stretching frequency (14 cm^{-1} compared with 1) demonstrates that this ligand is bonded to the rhodium(I) center as shown in Figures 5 and 8. Compound **6a** is unstable in solution and disproportionates to give precipitation of **7a** and reformation of 1. Such a phenomenon is not scarce and has been already observed, for example, with $Me_3IPt(\mu\text{-pypz})PtMe_2$.[42]

Addition of chlorine (by injection with a syringe) into a solution of 1 in CH_2Cl_2, with a ratio Cl_2:Rh = 1:2, leads to a green solution with simultaneous formation of a small amount of an orange precipitate, **6b**. Although the low solubility of **6b** precluded any NMR investigation, its infrared and analytical data allowed us to propose a formula and structure similar to that of **6a**.

By concentration of the green solution, a new compound, **8b**, was isolated. Redissolution of **8b** in methanol gave, through precipitation with PF_6^-, a green precipitate, **8b′**. The IR spectrum of compounds **8b** and **8b′** show C–O stretching frequencies around 2060 cm^{-1}, namely about 100 cm^{-1} above the frequency measured for the Rh(III)–Rh(I) mixed-valence dihalo complexes, **6a** and **6b**. Nevertheless, it is difficult to admit that the carbonyl is supported by

(42) Scott, J. D.; Puddephatt, R. J. *Organometallics* **1986**, *5*, 2522.

Table IX. $^{31}P\{^1H\}$ and ^1H NMR Data for the Bimetallic Neutral Complexes 9–11

compd	$\delta(^{31}P)$, ppm	J_{P-Rh}, Hz	$J_{P-Rh'}$, Hz	$\delta(^1H)$, ppm (for Cp and Me in C_7D_8)
$[Rh(I)(CpPPh_2)]_2$ (9a)	35.2 (AA'XX')	151.0[a]		6.7, 6.3, 5.8, 3.5 (8 H of Cp)
$[Rh(Cl)(CpPPh_2)]_2$ (9b)	41.6(AA'XX')	151.5[b]		6.7, 6.3, 5.7, 2.7 (8 H of Cp)
$[Rh(Me)(CpPPh_2)]_2$ (10a)	59.9(AA'XX')	179.0[c]		6.6, 6.2, 5.2, 4.0 (8 H of Cp), 0.425 (dd, J_1 = 2.64, J_2 = 6.45 Hz, 6 H of Me)
$[RhPh(CpPPh_2)]_2$ (10b)	47.5(AA'XX')	175.0[c]		7.0, 6.5, 4.0 (8 H of Cp)
$[Rh_2(I)(Me)(CpPPh_2)_2]$ (11)	55.4 (ddd)	180.9	8.8[d]	6.7, 6.6, 6.3, 6.1, 5.7, 5.4, 3.9, 3.1 (8 H of 2 Cp), 0.302 (dd, J_1 = 2.64, J_2 = 6.45 Hz, 3 H of Me)[d]

[a] In $CDCl_3/CHCl_3$. [b] In C_6D_6/CH_2Cl_2. [c] In CD_2Cl_2. [d] $J_{P-P'}$ = 4.4.[e] [e] In C_7D_8.

a rhodium(III) center (the C–O vibration in $[CpRh(CO)(PPh_3)Cl]^+$ lies above 2080 cm^{-1}). The $^{31}P\{^1H\}$ spectrum shows two signals as "doublet of doublets of doublets" of equal intensities with very similar $^1J_{P-Rh}$ (144.1 and 146.1 Hz), $^2J_{P-Rh}$ (7.2 and 4.5 Hz), and $^2J_{P-P'}$ (4.5 Hz). These observations argue strongly against different oxidation states of the metal atoms. In addition, the values of $^1J_{P-Rh}$ are inconsistent with rhodium(I) centers. Finally, the field desorption mass spectrometry shows the parent peak of a cationic species whose isotopic pattern and mass number do fit the formula $[Rh_2(CO)(Cl)(CpPPh_2)_2]^+$. Therefore, we describe the cationic part of **8b** and **8b'** as a Rh(II)–Rh(II) complex in which a metal–metal bond accounts for the diamagnetism and for the existence of a non-zero J_{P-P} coupling value (Figure 6).

In **8b**, the counterion is a chloride and therefore the observed slow transformation of this salt into **6b** is clearly a nucleophilic attack by Cl^- on the rhodium carrying the chlorine atom. Moreover if iodide is allowed to react with **8b** or **8b'**, compounds **6a** and **6c**, respectively, are formed rapidly. They were easily characterized by infrared and NMR spectroscopy, and **6c** appeared to be analogous to **6a** and **6b** but with iodine and chlorine ligands. The scheme in Figure 8 sums up our results on the oxidative addition of halogen.

Reactivity of the Dicationic Species $[Rh^{II}L(\mu\text{-}CpPPh_2)]^{2+}$ (L = CO (2a), Solvent Such as CH_2Cl_2 (2e)) with Halides. The nucleophilic attack of the halides X^- (X^- = Cl^-, I^-) on **2a** in the molar ratio X^-:Rh = 1:2 afforded the monocationic compounds $[Rh_2X(CO)(\mu\text{-}CpPPh_2)_2]^+$ (**8**), a type of compound previously exemplified by the case of the chloride **8b**. This compound **8b** has already been shown to react further with halide X^- to give the neutral $[X(Cl)Rh(\mu\text{-}CpPPh_2)RhCO]$ (**6b** or **6c**). In the absence of excess of halide, the use of the cationic species **2a** as starting material gives easy access to **8a** (X = I) and therefore offers the opportunity to generalize the pathway **1** → **8** → **6** (Figure 8), whatever the halogen may be.

In contrast with the reactions of **2a**, the solvated species $[Rh^{II}(solv)(CpPPh_2)]_2^{2+}$ (**2e**) reacts with halides to give *neutral dihalo* bimetallic complexes. The best way to prepare **2e** in situ consists of the oxidatin of the carbonyl ligands in **2a** with trimethylaminoxide, in solvents such as CH_2Cl_2 or acetone. Then the resulting green solution can be sifted for example through KI, affording a red solution, from which a red microcrystalline compound analyzing as $[Rh(I)(CpPPh_2)]_2$ (**9a**) was obtained. The dichoro analogue **9b** was prepared by the same method but, curiously, as a green product. The neutral dihalo compounds **9a** and **9b** show ^1H, ^{31}P (Table IX), and ^{13}C NMR spectra similar to those of the dicationic complexes **2** (Tables V and VI) and are probably of the same structural type (vide infra). The $^{31}P\{^1H\}$ spectrum consists of an AA'XX' signal with quite similar apparent J_{P-Rh} couplings for both products (151.0 and 151.5 Hz). The ^1H and ^{13}C spectra are also similar to those of compounds **2** and clearly differentiate the chemical situations of the four protons and of the five carbons in the two cyclopentadienyl ligands.

The reactions of the halides with the carbonyl **2a** and with the solvated **2e** compounds illustrate the subtle competition between metal–ligand and metal–metal bond cleavage after a nucleophilic attack. In both cases, the first step of the reaction is quite probably the electrophilic substitution of a terminal ligand on one of the 18-electron metal centers and in the case of **2e** this step is just repeated once more on the other metal center. In contrast, in the case of **2a**, the halide ligand introduced in the first step, polarizing the metal–metal bond, makes it more sensitive to heterolytic breaking than the metal–carbon bond of the carbonyl ligand on the second metal atom. In other words, the carbonyl protects the *second* metal atom from further nucleophilic attack. Such an overall situation favors the nucleophilic attack of the entering halide on the *first* metal center. Then, metal–metal bond breaking leads to a mixed-valence compounds **6**, associating a rhodium(III) and a rhodium(I) 18-electron center.

Syntheses of Dialkyl Dimetallic Complexes $[RhR(\mu\text{-}CpPPh_2)]_2$ (R = Me (10a), Ph (10b)): Preliminary Observations on a Polyhydrido Dimetallic System $[Rh(H)_n(\mu\text{-}CpPPh_2)]_2$. The dialkyl compounds **10a** and **10b** were easily obtained, in diethyl ether, by transmetalation reactions between the compound **9a** and either methyllithium or phenylmagnesium bromide, respectively. If very small amounts of methyllithium were used, then the intermediate monomethyl product $[Rh_2(\mu\text{-}CpPPh_2)_2(I)(Me)]$ (**11**) could be formed. The blue alkyl derivatives were characterized by chemical analysis, and ^1H and $^{31}P\{^1H\}$ NMR spectroscopy (Table IX). A ^{13}C NMR spectrum was also obtained for **10a**. Again, AA'XX' type ^{31}P spectra demonstrate the equivalence of the Rh–P moieties in these complexes. In the case of **11**, each phosphorus atom appeared in the $^{31}P\{^1H\}$ spectrum as a doublet of doublet of doublets, from which the values of the two Rh–P direct couplings were measured (180.9 and 169.1 Hz). Their slight difference is consistent with the identical formal oxidation states of the rhodium atoms. Their absolute values are, as expected, different from those observed in **9a** and **10a**.

Our studies on the formation of hydrides were performed by following current procedures. By adding a solution of $LiBEt_3H$ in toluene at −70 °C to a suspension of the brown tetraiodo compound **7a**, a red solution was obtained. Its ^1H NMR spectrum presented only one signal at high field (−13.20 ppm), appearing as a doublet of doublets, consistant with equivalent hydrido ligands coupled with both ^{103}Rh and ^{31}P nuclei (coupling constants equal to 36.8 and 27.9, respectively). The $^{31}P\{^1H\}$ sectrum appeared again as an AA'XX' system ($\delta(^{31}P)$ 53.83 ppm; J_{Rh-P} 170 Hz) demonstrating a symmetrical structure for a hydride $[Rh(H)_x(\mu\text{-}CpPPh_2)]_2$ (x = 1 or 2). Unfortunately, the product decomposed rapidly, giving a black intractable residue. When the diiodo compound **9a** was used under the same conditions, the ^1H NMR spectra showed several hydrido signals including the preceding one as a major

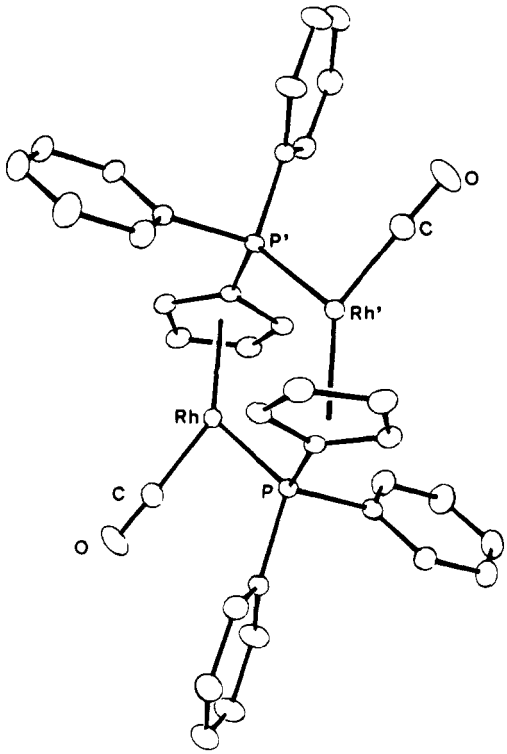

Figure 9. Perspective representation of the molecule $[Rh^{I}(\mu\text{-}CpPPh_2)(CO)]_2$ (**1a**) (reproduced from ref 1b).

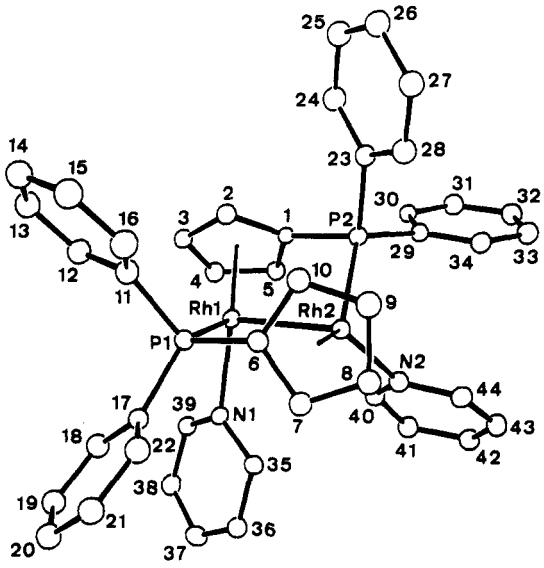

Figure 10. Perspective representation of the dicationic complex $[Rh^{II}(\mu\text{-}CpPPh_2)(pyridine)]_2^{2+}$ (**2b**).

component. In the $^{31}P\{^1H\}$ NMR spectrum, one of these hydrido complexes also showed an AA'XX' signal. The hypothesis that both the tetrahydrido ($x = 2$) and the dihydro ($x = 1$) complexes were formed is now under investigation.

Crystal Structures of the Compounds 2b, 5a', and 11. A Novel Type of Flexibility at the Bridging Ligand in Dimetallic Complexes. The molecular structure of 1 has already been solved[1a] and consists of two Rh(CO) moieties bridged by two (diphenylphosphino)cyclopentadienyl units in a mutual head-to-tail arrangement. The same disposition has also been found by Rausch, Atwood et al.[40] for the analogous (*dimethyl*phosphino)-cyclopentadienyl complex. We have reproduced in Figure 9 the ORTEP perspective view of 1. One can recall that the

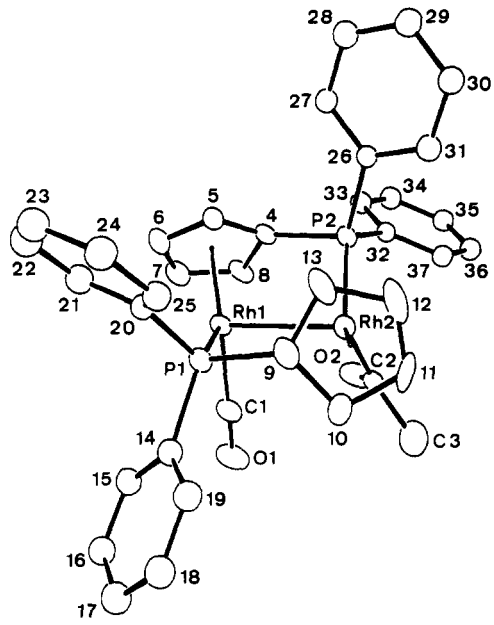

Figure 11. Perspective representation of the monocationic species $[(COCH_3)Rh^{II}(\mu\text{-}CpPPh_2)Rh^{II}(CO)]^+$ (**5a'**).

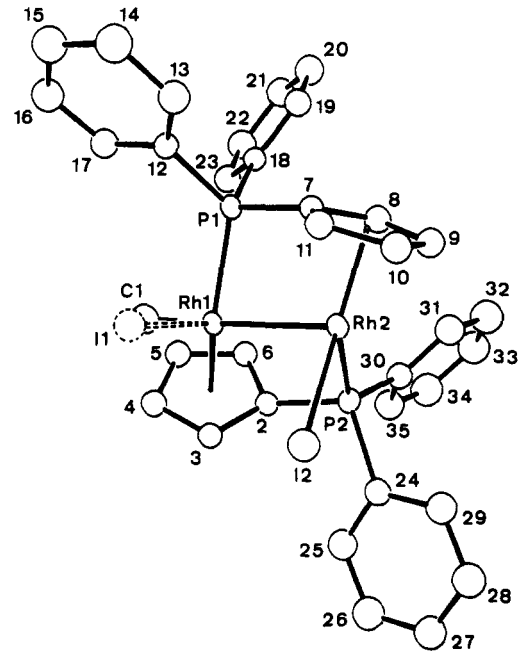

Figure 12. Perspective representation of the neutral species $[(H_3C)Rh^{II}(\mu\text{-}CpPPh_2)_2Rh^{III}I]$ (**11**).

geometry around each rhodium atom strongly resembles that around the iridium atom in $(\eta^5\text{-}C_5H_5)Ir(CO)(PPh_3)$.[43] A large metal–metal separation of 4.3029 (6) Å has been noted in 1, also we have recalculated 4.1656 (10) Å in $[RhCO(\mu\text{-}CpPMe_2)]_2$ from the data already published by Rausch et al.[40] A similar molecular structure is expected for the iridium analogue **12**.

The long rhodium–rhodium distance seems a priori to be imposed by the dimensions of the bridging units. In contrast, the fact that the d^7–d^7 compounds **2**, **5**, **8**, **10**, and **11** were diamagnetic quite naturally suggested the existence of metal–metal bond and thus arose the question of the possible deformations of this bridging unit with respect to the configuration observed in 1. Therefore X-ray

(43) Benett, M. J.; Prait, J. L.; Taygle, R. M. *Inorg. Chem.* **1974**, *13*, 2408.

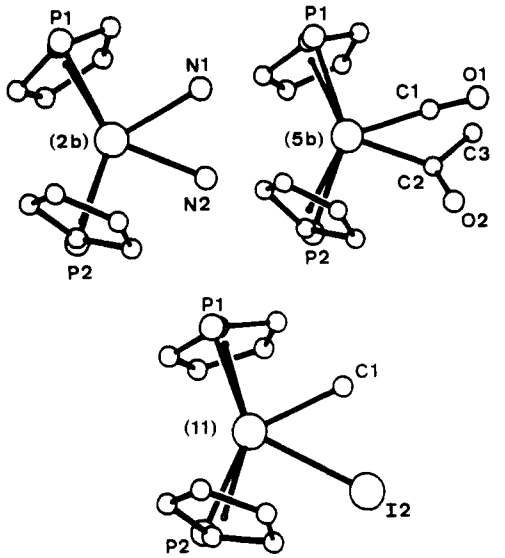

Figure 13. Cisoid disposition of the terminal ligands in the compounds **2b**, **5a′**, and **11** shown by projection along the Rh^{II}–Rh^{II} axis.

Table X. Selected Bond Lengths (Å) and Angles (deg) with Esd's in Parentheses for 2b

Rh(1)–Rh(2)		2.7796 (9)	
Rh(1)–P(1)	2.272 (2)	Rh(2)–P(2)	2.246 (2)
Rh(1)–N(1)	2.150 (6)	Rh(2)–N(2)	2.131 (7)
Rh(1)–Cp(1)	1.871 (4)	Rh(2)–Cp(2)	1.878 (6)
Rh(1)–C(1)	2.166 (5)	Rh(2)–C(6)	2.206 (6)
Rh(1)–C(2)	2.163 (5)	Rh(2)–C(7)	2.253 (5)
Rh(1)–C(3)	2.247 (4)	Rh(2)–C(8)	2.273 (5)
Rh(1)–C(4)	2.301 (5)	Rh(2)–C(9)	2.238 (6)
Rh(1)–C(5)	2.253 (5)	Rh(2)–C(10)	2.196 (6)
Rh(2)–Rh(1)–P(1)	77.37 (5)	Rh(1)–Rh(2)–P(2)	77.74 (6)
Rh(2)–Rh(1)–N(1)	101.8 (2)	Rh(1)–Rh(2)–N(2)	99.5 (2)
Rh(2)–Rh(1)–Cp(1)	110.4 (2)	Rh(1)–Rh(2)–Cp(2)	110.4 (2)
P(1)–Rh(1)–N(1)	92.3 (2)	P(2)–Rh(2)–N(2)	89.9 (2)
P(1)–Rh(1)–Cp(1)	132.4 (2)	P(2)–Rh(2)–Cp(2)	130.3 (2)
N(1)–Rh(1)–Cp(1)	128.7 (2)	N(2)–Rh(2)–Cp(2)	133.3 (2)
P(1)–C(6)	1.799 (6)	P(2)–C(1)	1.803 (5)
P(1)–C(11)	1.782 (7)	P(2)–C(23)	1.833 (6)
P(1)–C(17)	1.795 (5)	P(2)–C(29)	1.818 (5)
N(1)–C(35)	1.352 (9)	N(2)–C(40)	1.346 (11)
C(35)–C(36)	1.388 (11)	C(40)–C(41)	1.385 (13)
C(36)–C(37)	1.369 (13)	C(41)–C(42)	1.396 (12)
C(37)–C(38)	1.408 (10)	C(42)–C(43)	1.377 (13)
C(38)–C(39)	1.383 (12)	C(43)–C(44)	1.390 (14)
C(39)–N(1)	1.336 (1)	C(44)–N(2)	1.360 (11)
Rh(1)–N(1)–C(35)	120.2 (5)	Rh(2)–N(2)–C(40)	120.3 (5)
Rh(1)–N(1)–C(39)	120.4 (4)	Rh(2)–N(2)–C(44)	118.7 (6)
C(35)–N(1)–C(39)	118.9 (7)	C(40)–N(2)–C(44)	120.9 (8)
N(1)–C(35)–C(36)	120.2 (7)	N(2)–C(40)–C(41)	121.3 (8)
C(35)–C(36)–C(37)	119.0 (7)	C(40)–C(41)–C(42)	118.5 (9)
C(36)–C(37)–C(38)	119.6 (8)	C(41)–C(42)–C(43)	119.2 (9)
C(37)–C(38)–C(39)	117.9 (8)	C(42)–C(43)–C(44)	120.6 (8)
C(38)–C(39)–N(1)	121.2 (6)	C(43)–C(44)–N(2)	119.2 (8)

[a] Cp(1) and Cp(2) are the centroids of the cyclopentadienyl rings [C(1)C(2)C(3)C(4)C(5)] and [C(6)C(7)C(8)C(9)C(10)], respectively.

crystallographic investigations of suitable crystals of the dicationic **2b**, monocationic **5a′**, and neutral **11** species were carried out. Figures 10–12 give for each compound an ORTEP perspective view, while projections along the metal–metal axes are compared in Figure 13. Selected bond lengths and angles are given in Tables X–XII.

For the three cases, a striking similarity between the structures appears. The head-to-tail disposition of the bridging ligands is similar to that observed in **1**, but the conformation of the $[(\mu\text{-CpPPh}_2)\text{Rh}]_2$ moiety has changed drastically. The new conformation in the three cases (Figures 10–13) can be readily contrasted with that in **1** (Figure 9). Particularly, the transoid mutual disposition of the terminal ligands in **1** gives place to cisoid ones in

Table XI. Selected Bond Lengths (Å) and Angles (deg with Esd's in Parentheses for 5a′[a]

Rh(1)–Rh(2)		2.7319 (6)	
Rh(1)–Cp(1)	1.890 (5)	Rh(2)–Cp(2)	1.890 (7)
Rh(1)–C(1)	1.893 (7)	Rh(2)–C(2)	2.004 (7)
Rh(1)–P(1)	2.273 (2)	Rh(2)–P(2)	2.245 (1)
Rh(2)–Rh(1)–Cp(1)	108.2 (2)	Rh(1)–Rh(2)–Cp(2)	111.5 (2)
Rh(2)–Rh(1)–C(1)	91.7 (2)	Rh(1)–Rh(2)–C(2)	94.3 (2)
Rh(2)–Rh(1)–P(1)	76.84 (4)	Rh(1)–Rh(2)–P(2)	80.46 (4)
Cp(1)–Rh(1)–C(1)	131.4 (3)	Cp(2)–Rh(2)–C(2)	129.4 (3)
Cp(1)–Rh(1)–P(1)	133.9 (2)	Cp(2)–Rh(2)–P(2)	133.3 (2)
C(1)–Rh(1)–P(1)	93.1 (2)	C(2)–Rh(2)–P(2)	92.2 (2)
Rh(1)–C(4)	2.256 (5)	Rh(2)–C(9)	2.215 (6)
Rh(1)–C(5)	2.180 (5)	Rh(2)–C(10)	2.227 (7)
Rh(1)–C(6)	2.269 (6)	Rh(2)–C(11)	2.238 (8)
Rh(1)–C(7)	2.254 (6)	Rh(2)–C(12)	2.245 (6)
Rh(1)–C(8)	2.232 (5)	Rh(2)–C(13)	2.265 (6)
C(1)–O(1)	1.095 (9)	C(2)–O(2)	1.115 (9)
C(2)–C(3)		1.438 (10)	
Rh(1)–C(1)–O(1)	174.3 (6)	Rh(2)–C(2)–C(3)	117.1 (5)
Rh(2)–C(2)–O(2)	124.4 (5)	O(2)–C(2)–C(3)	117.7 (7)
P(1)–C(9)	1.778 (7)	P(2)–C(4)	1.799 (6)
P(1)–C(14)	1.811 (4)	P(2)–C(26)	1.809 (4)
P(1)–C(20)	1.794 (4)	P(2)–C(32)	1.816 (4)
C(4)–C(5)	1.415 (8)	C(9)–C(10)	1.463 (9)
C(5)–C(6)	1.403 (9)	C(10)–C(11)	1.427 (10)
C(6)–C(7)	1.356 (9)	C(11)–C(12)	1.344 (11)
C(7)–C(8)	1.432 (10)	C(12)–C(13)	1.401 (10)
C(8)–C(4)	1.446 (7)	C(13)–C(9)	1.408 (8(
C(8)–C(4)–C(5)	105.5 (5)	C(13)–C(9)–C(10)	107.3 (6)
C(44)–C(5)–C(6)	110.0 (5)	C(9)–C(10)–C(11)	105.1 (6)
C(5)–C(6)–C(7)	107.6 (6)	C(10)–C(11)–C(12)	109.7 (6)
C(6)–C(7)–C(8)	110.3 (6)	C(11)–C(12)–C(13)	110.4 (6)
C(7)–C(8)–C(4)	106.2 (5)	C(12)–C(13)–C(9)	107.5 (6)
P(2)–C(4)–C(5)	125.9 (4)	P(1)–C(9)–C(10)	123.2 (5)
P(2)–C(4)–C(8)	123.3 (5)	P(1)–C(9)–C(13)	125.4 (5)
P(2)–C(4)–Rh(1)	105.3 (2)	P(1)–C(9)–Rh(2)	102.7 (3)

[a] Cp(1) and Cp(2) are the centroids of the cyclopentadienyl rings [C(4)C(5)C(6)C(7)C(8)] and [C(9)C(10)C(11)C(12)C(13)], respectively.

Table XII. Selected Bond Lengths (Å) and Angles (deg) with Esd's in Parentheses for 11[a]

Rh(1)–Rh(2)		2.7160 (7)	
Rh(1)–P(1)	2.206 (2)	Rh(2)–P(2)	2.244 (2)
Rh(1)–Cp(1)	1.889 (5)	Rh(2)–Cp(2)	1.874 (6)
Rh(1)–C(1)	2.11 (1)	Rh(2)–I(2)	2.6622 (7)
Rh(1)–I(1)	2.75 (1)		
Rh(2)–Rh(1)–P(1)	79.10 (5)	Rh(1)–Rh(2)–P(2)	76.54 (5)
Rh(2)–Rh(1)–Cp(1)	112.5 (1)	Rh(1)–Rh(2)–Cp(2)	110.4 (1)
Rh(2)–Rh(1)–C(1)	94.8 (3)	Rh(1)–Rh(2)–I(2)	95.63 (3)
P(1)–Rh(1)–Cp(1)	141.3 (1)	P(2)–Rh(2)–Cp(2)	139.1 (2)
P(1)–Rh(1)–C(1)	87.0 (3)	P(2)–Rh(2)–I(2)	91.56 (5)
Cp(1)–Rh(1)–C(1)	126.3 (3)	Cp(2)–Rh(2)–I(2)	126.1 (1)
Rh(1)–C(2)	2.214 (5)	Rh(2)–C(7)	2.182 (5)
Rh(1)–C(3)	2.214 (5)	Rh(2)–C(8)	2.215 (5)
Rh(1)–C(4)	2.252 (5)	Rh(2)–C(9)	2.267 (6)
Rh(1)–C(5)	2.276 (5)	Rh(2)–C(10)	2.267 (5)
Rh(1)–C(6)	2.253 (5)	Rh(2)–C(11)	2.215 (6)
P(1)–C(7)	1.809 (5)	P(2)–C(2)	1.804 (5)
P(1)–C(12)	1.817 (6)	P(2)–C(24)	1.811 (6)
P(1)–C(18)	1.823 (5)	P(2)–C(30)	1.821 (7)

[a] Cp(1) and Cp(2) are the centroids of the cyclopentadienyl rings [C(2)C(3)C(4)C(5)C(6)] and [C(7)C(8)C(9)C(10)C(11)], respectively.

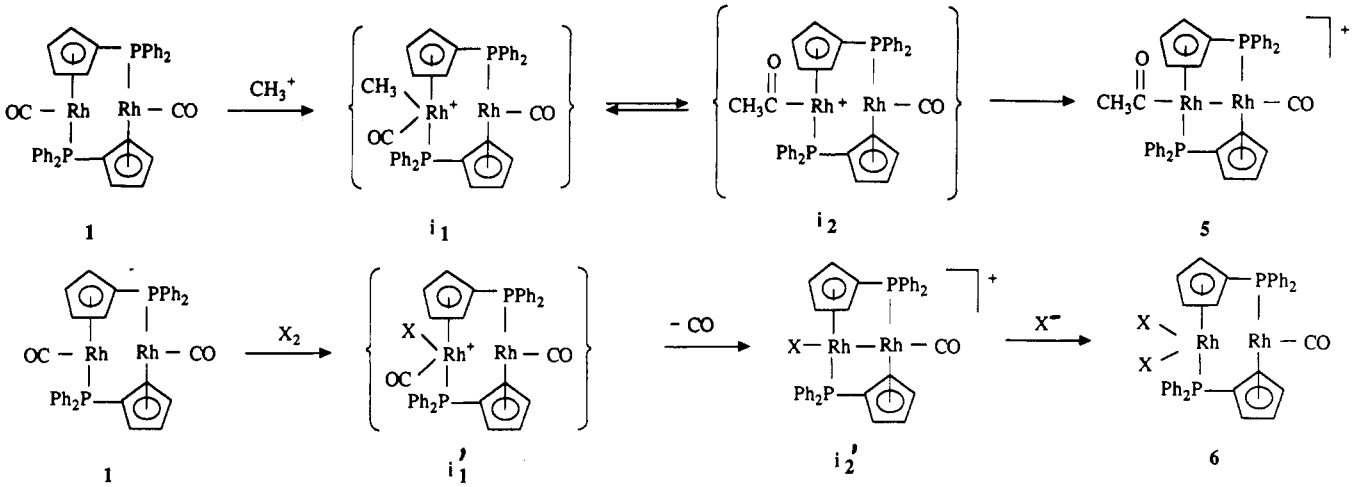

Figure 14. (a, Top) alkyl migration promoted intramolecularly by metal–metal interaction. (b, Bottom) electrophilic substitution promoted by metal–metal interaction.

2b, **5a′**, and 11. Moreover the new structures allow remarkable shortening of the rhodium–rhodium distances from 4.3029 (6) Å in 1 to 2.7796 (9) Å in **2b**, 2.7319 (6) Å in **5a′**, and 2.7160 (7) Å in 11, demonstrating, as expected for these d^7–d^7 species, the formation of a metal–metal single bond. One can note also the decreasing values of this bond along the series from the dication to the neutral species.

From the above results, we assume the same disposition in all the d^7–d^7 species that we have prepared. The novel type of flexibility offered by the Cp–PR_2 2-fold bridging unit is primarily understood as the result of two possible rotations along two almost perpendicular axis, viz. the Rh–Cp axis and the Cp–P axis. The angles C(Cp)–P–Rh along the series are almost constant, varying approximately from 130 to 140°. The phosphorus atoms are shifted from the mean planes of the cyclopentadienyl toward the rhodium atoms, by approximately 0.5 Å.

These observations emphasize the quite interesting function of the $[\mu\text{-CpPR}_2]_2$ unit, working as a "ball and socket joint" between the two molecular moieties and thus allowing very large variations of the metal–metal distance.[44] In the absence of experimental evidence favoring either the breaking of the bridged structure or the slippage of the cyclopentadienyl ligand, we must assume that this new type of deformation of the bridging unit composed of two rotations around the C(Cp)–P and P–Rh bonds is a continuous process. It is interesting to note that mimicking such a deformation is easy using a "ball and stick" molecular model.

This hypothesis can been used to describe the reaction of 1 with CH_3I. In this case it is reasonable to assume that the primary step consists of a rapid attack of the carbocation CH_3^+ at one rhodium atom, leading to an intermediate i_1 (Figure 14a). Such an intermediate has been obtained in the reaction of the dinuclear complex $[CpRh(CO)]_2(\mu\text{-dpdp})$ with methyl triflate.[21] It is well-known that the methyl carbonyl intermediates such as i_1 are in equilibrium with a coordinatively unsaturated acyl form[22] such as i_2 (or solvated).

In our case, these intermediates have not been detected; they transform readily into **5** under the stabilizing effect of the metal–metal bond formation. Actually, in Figure 14a we have assumed that the facile conformational change of the bridging unit takes place at the last step of the mechanism. To our knowledge, this is the second example, after the result reported by Collman et al.[45] of an alkyl migration promoted intramolecularly by metal–metal interaction. In Figure 14b is proposed a possible mechanism for the oxidative addition of halogens emphasizing the analogous role of metal–metal bond formation at the second step (i'_1 to i'_2), which can be considered as a metal–metal promoted process.

The "ball and socket joint" effect of the $(CpPR_2)_2$ bridging unit presumably plays an important role in the oxidation processes of 1. It will be interesting to learn more about it by electrochemical studies, and such studies are underway. By using other metals, it will also be possible to modulate the effect of the metal–metal bond. Finally, the unique cisoid disposition of the terminal ligands (Figure 13) calls for further studies of intermetallic processes.

Supplementary Material Available: For compounds **2b** and 11, tables of hydrogen atom positional and thermal parameters, anisotropic thermal parameters, and bond lengths and angles (7 pages); listings of the structure factors (44 pages). Ordering information is given on any current masthead page.

(44) Such large variations of metal–metal distance are also observed when thiolates are used as bridging ligands. In the series of trinuclear "crownlike" compounds based on a $[Ir(\mu\text{-SR})]_3$ skeleton, sulfur was shown to admit a large variation of the Ir–S–Ir angle and subsequently to accommodate Ir–Ir distances as different as 2.7 or 4.2 Å (Devillers, J.; de Montauzon, D.; Poilblanc, R. *New. J. Chem.* **1983**, *7*, 545).

(45) (a) Collman, J. P.; Rothrock, R. K.; Finke, R. G.; Rose-Munch, F. *J. Am. Chem. Soc.* **1977**, *99*, 7381. (b) Collman, J. P.; Rothrock, R. K.; Finke, R. G.; Moore, E. J.; Rose-Munch, F. *Inorg. Chem.* **1982**, *21*, 146. (c) Shyn, S. G.; Wojcicki, A. *Organometallics* **1985**, *4*, 1457.